In presenting this thesis in partial fulfillment of the requirements for an advanced degree at Idaho State University, I agree that the Library shall make it freely available for inspection. I further state that permission to download and/or print my thesis for scholarly purposes may be granted by the Dean of the Graduate School, Dean of my academic division, or by the University Librarian. It is understood that any copying or publication of this thesis for financial gain shall not be allowed without my written permission.

Signature ___________________________________

Date _______________________________________

VEGETATION MEASUREMENTS IN SAGEBRUSH STEPPE USING TERRESTRIAL LASER SCANNING

by

Kyle Anderson

A thesis submitted in partial fulfillment of the requirements for the degree of

Master of Science in the Department of Geosciences

Idaho State University

Fall 2014

To the Graduate Faculty:

The members of the committee appointed to examine the thesis of KYLE E ANDERSON find it satisfactory and recommend that it be accepted.

Dr. Donna M. Delparte,
Major Advisor

Dr. Nancy Glenn,
Committee Member

Dr. Douglas J. Shinneman,
Committee Member

Dr. DeWayne R. Derryberry,
Graduate Faculty Representative

Acknowledgements

This work would have been impossible without the support and encouragement of my mentors, collaborators, and colleagues. I have benefited a great deal from these relationships and am deep in the debt of many.

First I thank my advisor, Dr. Nancy Glenn. Without her sage advice, patience, good cheer, and unflappable determination, this project may have foundered on any one of many challenges. Nancy gave me every intellectual, logistical, and personal support while allowing me creativity and discretion in my work. I am honored to have been included in Nancy's academic enterprise and I have learned an immense amount because of it. I hope that this and future work will do some justice to her investment of time and energy.

I thank Lucas Spaete, who served as a mentor and steady coworker throughout the project. Lucas's optimism, experience, and technical know-how was indispensable in every step of my work. Where my ideas failed, Lucas's generally succeeded. Likewise I thank Dr. Rupesh Shrestha and Peter Olsoy for countless expert consults. I would have been utterly lost without these competent, patient, and good-humored colleagues.

I thank Kyle Gochner, Sam Gould, Dr. Aihua Li, Shital Dhakal, and Timothy Phero for working alongside me in the field, and for cheerfully enduring my imperfect direction in addition to hard effort in hot weather. I am proud of the amount of data we were able to collect together.

I thank my collaborators at the USGS Forest and Range Ecosystem Science Center—Drs. Douglas Shinneman, Robert Arkle, David Pilliod, Susan McIlroy—for their logistical and intellectual support, and patience in arranging coordinated data collection and analysis. I am excited to have played a small part in their work to understand and conserve imperiled rangeland ecosystems.

I thank my advisory committee—Drs. Nancy Glenn, Donna Delparte, DeWayne Derryberry, and Douglas Shinneman—for their patience, guidance, and encouragement. My efforts required diverse corrections and I feel blessed to have had this rounded group of experts checking my work.

Finally I thank the USGS (Joint Fire Sciences Program Award, *Quantifying and predicting fuels and the effects of reduction treatments along successional and invasion gradients in sagebrush habitats*) and the NOAA OAR Earth Systems Research Laboratory/ Physical Sciences Division (Award NA10OAR4680240) for funding this project. I hope my work's contribution to scientific knowledge and conservation goals merits the faith that was put in me.

Other faculty, fellow researchers, fellow students, family, and friends who helped me through this experience are too many to list. I sincerely thank all who had a role in seeing this project through.

Table of Contents

List of Tables

List of Figures

VEGETATION MEASUREMENTS IN SAGEBRUSH STEPPE USING TERRESTRIAL LASER SCANNING

Thesis Abstract – Idaho State University (2014)

Terrestrial laser scanning (TLS) enables efficient collection of vegetation structural characteristics across large swaths, and may provide a valuable tool for research and management efforts in sagebrush-dominated rangeland ecosystems in the western United States. We studied the use of TLS in rangeland environments at the scale of hectare plots (n = 26). First, we tested the ability of TLS-derived measurements of structure to model canopy cover and biomass of several classes of vegetation, using manually collected data from 1 x 1 m quadrats (n = 206) for training and validation. We applied Random Forests regression modeling to predict canopy cover and biomass of different vegetation classes using TLS-derived structural properties, with model strength ranging between $R^2 = 0.28$ and $R^2 = 0.72$. Second, we performed several experiments to quantify occlusion in TLS point clouds collected in rangelands and the success of methods to mitigate it, providing a body of useful information to optimize the efficiency and quality of future TLS collections in rangelands.

Chapter 1. Purpose and Background

1.1. Statement of Purpose

Dryland ecosystems, which cover over 40% of Earth's land area (White and Nackoney 2003), are susceptible to numerous sources of degradation. Prominent among these are mismanaged grazing (Milton et al. 1994), biological invasion (D'Antonio and Vitousek 1992), anthropogenic alteration of fire regimes (Bistinas et al. 2013), changing climate (Cowie et al. 2011), and human land use (Reynolds et al. 2007). Degradation of dryland ecosystems often yields consequences that fit a pattern termed "desertification". Deleterious effects of desertification include soil loss (Ravi et al. 2010), increased wildfire hazard (D'Antonio and Vitousek 1992), decreased carbon storage (White and Nackoney 2003), reduced forage quality (Milton et al. 1994), reduced ecosystem complexity (Cowie et al. 2011), negative impacts on air quality (Goudie 2014), negative impacts on water quality (Bregas 1998), and loss of cultural value (Reynolds et al. 2007). An estimated 10% - 20% of Earth's drylands are affected by desertification (WRI 2005).

Shrub ecosystems occupy more than half of Earth's drylands (Reynolds et al. 2007), including approximately 47 million hectares of sagebrush (*Artemisia tridentata*) - dominated steppe in the western United States (Bukowski and Baker 2013). Native sagebrush-steppe plant communities are composed of various shrub species, bunchgrasses, forbs, and biological crust constituents (Davies and Bates 2010). The diverse fauna occupying sagebrush-steppe include several obligate wildlife species, notably the charismatic sage grouses (*Centrocercus sp.*) and pygmy rabbit (*Brachylagus idahoensis*) (Welch 2005). Human land uses in sagebrush-steppe include ranching, recreation, cultural, and military (Knick et al. 2011), and ecosystem services include carbon storage and sequestration (Hunt et al. 2004) and capture of snow, nutrients, and sediments (e.g. Sankey et al. 2012).

It is estimated that sagebrush-steppe ecosystems currently occupy about 55% of their historical range in the western United States. About 13% of this range has been converted to agriculture, and about 1% is occupied by urban areas or human infrastructure. The remainder is occupied by non-shrubland ecosystems, typically dominated by non-native species, but including to a lesser extent areas where native woodlands have encroached onto shrublands (Knick et al. 2004). The replacement of native shrub-dominated communities by non-native plants is largely driven by a phenomenon referred to as the "grass-fire cycle", wherein the presence of invasive annual grass and forb species promote more frequent and severe wildfires, which in turn encourage the further spread and dominance of non-native plants (D'Antonio and Vitousek 1992). The invasive grass-fire cycle often introduces a desertified ecological steady-state, with little hope of reestablishing native communities (Knick 1999). A separate dynamic exists in montane areas, where livestock grazing, fire suppression, and periods of above-average moisture have allowed native conifer woodlands to encroach on adjacent shrub-steppe. The encroachment of conifers into shrublands increases coarse woody fuels and enhances the risk of severe stand-replacing fires, which may also result in invasion by non-native annual plant species and potential transition to a grass-fire cycle (Miller and Tausch 2000).

The dire degradation threats in the steppes of the western United States have prompted urgent management efforts, including legislation mandating the preservation and rehabilitation of sagebrush-steppe and prevention of future catastrophic wildfires (e.g. Federal Land Assistance, Enhancement, and Management Act 2009, Healthy Lands Initiative 2009). Different landscape treatments endorsed and carried out in support of these goals include the planting of tall, deep-rooted bunchgrasses to compete with invasive plants, fuels reduction via strategic grazing, wildfire suppression, invasive plants eradication via herbicide or controlled burns (Johnson and Davies 2012), mechanized thinning of dense shrub communities and removal of encroaching trees (Davies et al. 2012), and planting of fire-resistant "greenstrips" (Davison and Smith 1997). However, understanding the long-term efficacy of these treatments requires further study (Beck et al. 2009, Davies et al. 2012, Hess and Beck 2012).

The ability to inventory the quantity and makeup of rangeland vegetation is essential to target landscape treatments and understand their effects, in addition to a host of ecological modeling purposes. Historical efforts to take stock of rangeland vegetation have relied on field-measured metrics, such as transect and frame-based measurements in plot-scale studies (Davies et al. 2012), and harvested dry weight and various volume derivations for studies at the scale of individual plants (Uresk et al. 1977). These manual methods are accurate, but limited in scope by manpower and logistics (Bonham 1989).

Remote sensing technology offers the ability to extend measurements of vegetation traits across the vast and often-remote rangeland landscapes of the western United States. However, interpretation of spectral data is challenged by the small stature, mute color, and sparse canopies of individual plants, and their sparse arrangement across the landscape, so application of spectral remote sensing towards shrub-steppe inventory has largely been limited to qualitative mapping of broad ecosystem types (Jacobson and

Snyder 2000, Knick et al. 1997, Sankey and Germino 2008, Okin et al. 2001). Fusion of spectral data with structural information derived from airborne laser scanning (ALS) has the potential to improve classification to the community or species level, and also offers a means of quantifying the stature of vegetation (Bork and Su 2007, Mundt et al. 2006, Sankey et al. 2010). The utility of ALS is somewhat limited by the low point density and high error of typical collections, relative to low-stature shrubs and herbaceous rangeland vegetation (Mitchell et al. 2011, Sankey and Bond 2011, Streutker and Glenn 2006).

Terrestrial laser scanning (TLS) allows structural measurements at centimeter resolution over ranges extending to hundreds of meters, and provides an intermediate approach between highly-localized, precise field measurements and spatially-extensive, relatively-coarse remotely-sensed measurements from aerial and satellite platforms. Applications of high-definition TLS collection to inventory of sagebrush-steppe include work to predict biomass of individual sagebrush shrubs (Olsoy et al. 2014a, b), model 2 cm scale structure of individual sagebrush shrubs (Adams 2014), detect individual shrubs across plots, and predict their height and crown area (Vierling et al. 2013). In a similar shrub-dominated ecoystem, TLS has been demonstrated to predict the volume of herbaceous and shrub fuelbeds (Loudermilk et al. 2009). Measurements made using TLS in sagebrush-steppe have also been strongly correlated with aerial laser scanning measurements, suggesting that TLS collections may be used to train and evaluate interpretation of broader-scale datasets (Li, in review).

This thesis research aims to build on the growing body of work applying TLS to rangeland inventory by developing methods to predict traits of different sagebrush-steppe vegetation types across hectare plots, with specific objectives to: (1) test the ability of

TLS-derived structural indices to predict field measurements of canopy cover and biomass of several classes of rangeland vegetation; (2) assess the repeatability of datasets yielded by a TLS sampling methodology in rangelands; (3) identify limitations and methods to optimize future applications of TLS in sagebrush-steppe.

1.2. Laser Scanning

Laser scanning, commonly called light detection and ranging (LiDAR), refers to technologies using laser pulse ranging measurements to record precise structural information about targets. Nearly all outdoor laser scanning systems operate by emitting a pulse of light in a known direction, and recording the time-of-flight between pulse emission and return, allowing calculation of the point in 3D space where the pulse was reflected. Additional information may be recorded about the amplitude of the light wave returning to the sensor, which may be used to infer properties of the target such as width, aspect, or spectral reflectance at the laser wavelength. Measuring the changing amplitude of the light wave returning to the sensor over time may allow inference of more than one 3D point per pulse release, as several peaks in the amount of returning energy may indicate fractions of the pulse reflecting off of several spatially-staggered surfaces falling in the bounds of the pulse's footprint. As the footprint of light pulses increase with range, the precision of measurements on the plane normal to the pulse path decreases accordingly, and the likelihood of a single target reflecting only a portion of the pulse's energy increases. Lasers of various wavelengths and powers may be deployed depending on the application (for example, green lasers penetrate water well and are useful to measure bathymetry, while near-infrared lasers are eye-safe and transmit well over long distances through air) and several lasers of different wavelengths employed on a single instrument allow for multispectral as well as structural sampling. Laser scanners may be deployed on static terrestrial, mobile terrestrial, airborne, and spaceborne platforms, with a variety of different mechanisms to achieve scanning action and, if necessary, account for platform motion (Heritage and Large 2009, Shan and Toth 2008).

Of the various configurations of laser scanners, ALS is the most common and mature, with diverse applications in vegetation studies. Use of ALS is especially well-established for inventory in forest environments, where the large size of trees enables collection of numerous samples per individual plant while sampling at typical point densities (4 - 15 measurements per m^2) (Wulder et al. 2012). ALS collections in forests have been used to effectively measure or predict diverse vegetation structural characteristics at the scale of both plots and individual trees, including height, canopy volume, basal area, and aboveground biomass (e.g. Andersen et al. 2005, Bork and Su 2007, Vierling et al. 2008). However, applications of ALS to vegetation structure inventory in shrub-dominated ecosystems have proven problematic due to low measurement accuracy, low sampling density, and large pulse footprints relative to small-stature shrubland vegetation. In particular, ALS measurements of height yield systematic negative errors where sampling density is too low to reliably sense small canopy peaks, or where canopy peaks are too small to reflect a greater proportion of pulse footprints than dense vegetation lower in the plant (Hopkinson et al. 2005, Sankey and Bond 2011). Increasing sampling density of collections has been shown to increase the accuracy of shrub structural measurements (Estornell et al. 2011), but even in optimal collections (high sampling density, low footprint size), error of ~30% in sagebrush height measurements were found to be routine (Mitchell et al. 2011). Even presence-absence predictions of sagebrush distribution were found to be mediocre using ALS as a standalone data source (Streutker and Glenn 2006). The ability of ALS collections to quantify non-shrub rangeland vegetation types has so far been hamstrung by measurement error, which often exceeds the total height of grasses and other annual herbaceous vegetation (Hopkinson et al. 2005, Streutker and Glenn 2006), although rapidly-improving sensor technology may overcome this limitation (Vierling et al. 2013).

TLS collections overcome some of the limitations presented by ALS. Consisting of a rotating scanner mounted on an elevated platform, TLS instruments provide rapid collection of super-dense sampling within the scanner's field of view, extending to ranges beyond a kilometer. The error of TLS measurements is low, and sampling at functionally-redundant density is often achievable at little logistical expense. While ALS sampling is limited to the topmost surfaces of targets (or a number of staggered upper surfaces, in the common case of multiple-return collections), TLS instruments may be deployed to collect from any angle—beyond the standard configuration of scanning horizontally from eye-level bases, TLS collections have been performed from extendable masts (USA ERDC 2012), canyon edges (Vierling et al. 2013), and in upward-scanning configurations (Zhao et al. 2012). Collections from several positions may be co-registered, allowing sampling of targets from diverse angles. The advantages provided by TLS come at a cost: while ALS collections offer roughly uniform sampling density, coverage, and range effects throughout the dataset, raw TLS point clouds are irregular, with sampling density and pulse footprint compactness decreasing exponentially with range from the scanner, and often-extensive unsampled ("shadowed") spaces where protruding surfaces occlude the instrument's field-of-view (Van der Zande 2008).

Predicting vegetation traits that cannot be directly measured using TLS point clouds is done using a variety of proxy measurements such as modeled plant volume or moving-window statistical measures of reflection positional distribution (e.g. range of sample heights, density of samples). Where range effects may be negated or normalized, the amplitude (intensity) of individual reflections has been shown to accurately discern fine fuels from coarse branchwood and green from woody vegetation (Olsoy et al. 2014, Seielstad et al. 2011). Different vegetation types may also be classified using structural indices, such as moving-window eigenvalues or similarity to a predetermined 3D "wavelet" shape (Brodu and Lague 2012, Garrity et al. 2012, Vierling et al. 2013).

A growing body of work employs TLS sampling to measure and predict a wide variety of vegetation characteristics. In forest ecosystems, TLS has been found to be an efficient replacement of traditional sampling methods in measuring a variety of common metrics including tree strem count, basal area, biomass, height, location, leaf area index, plant area index, and canopy gap fraction (Henning and Radtke 2006, Yao et al. 2011, Zhao et al. 2011, Zhao et al. 2012). Many of the applications of TLS towards shrubland research have been performed at the scale of individual plants, both in the field and as isolated laboratory specimens. These include measurement of fine-scale sagebrush structure for wildfire modeling purposes (Adams 2014), modeling of sagebrush biomass separated into green and woody classes (Olsoy et al. 2014b), measurement of shrub volume and limb surface area (Kaluza et al. 2012), and shrub leaf surface area (Loudermilk et al. 2009). At the plot scale, TLS has been used to measure sagebrush height and canopy area, model shrub and herbaceous fuelbed volume (Loudermilk et al. 2009), train sagebrush biomass modeling using ALS datasets (Li, in review), and create “fearscape” models of visibility through sagebrush cover (Olsoy, in press). Although we are unaware of research applying TLS-derived structural information towards non-shrub rangeland plant types (low grasses, tall bunchgrasses, and forbs), the success of past work using manual measurements of structure to estimate biomass of bunchgrasses suggests that it is possible (Andariese and Covington 1986, Tausch 1989).

1.3. Sagebrush-Dominated Ecosystems

Sagebrush ecosystems cover 47 million hectares in the western United States and are the dominant native landcover in drylands of the Great Basin and Columbia Basin (Bukowski and Baker 2013). Big sagebrush (*Artemisia tridentata*), which is the most common and widespread canopy species, is composed of 3 subspecies: Wyoming big sagebrush (*A. tridentata wyomingensis*) occupies relatively dry lowlands; mountain big sagebrush (*A. tridentata vasyana*) occupies relatively cool and mesic uplands; basin big sagebrush (*A. tridentata tridentata*) occupies intermediate environments (Tausch 1989). Allied shrub species include three other sagebrushes, low sagebrush (*A. arbuscula*), black sagebrush (*A. nova*), and rigid sagebrush (*A. rigida*), as well as bitterbrush (*Purshia tridentata*), snowberry (*Symphoricarpos sp.*), shadscale (*Atriplex confertifolia*), and rabbitbrush (*Chrysothamnus sp.*). The canopies of sagebrush ecosystems range from 30-200 cm high, and tend to have significant gaps, with interstitial spaces either left bare or occupied by a diversity of grasses and forbs ranging up to 60 cm high. These prominently include Idaho fescue (*Festuca idahoensis*), bluebunch wheatgrass (*Pseudoroegneria spicata*), needlegrasses (*Stipa sp.*), California brome (*Bromus carinatus*), squirreltail (*Sitanion hystrix*), and Sandberg’s bluegrass (*Poa secunda*). Site-level plant diversity ranges from 13 species in hot, xeric lowlands, up to 56 species in relatively mesic uplands (Miller and Eddleman 2000). The plant community is often underlain by a layer of biological crust (Knick et al. 2004, Miller and Eddleman 2000).

The climate of sagebrush ecosystems is highly variable, with significant effects on year-to-year abundance and diversity of herbaceous vegetation. Wildfire is a characteristic disturbance of most sagebrush ecosystems, but data is lacking to reconstruct historical fire regimes with great accuracy in many of these ecosystems (Baker 2011). Mean fire return intervals likely varied widely among different sagebrush communities, and have been estimated to range from a few decades (Miller and Heyerdahl 2008) to well over 200 years (Bukowski and Baker 2013). Historical wildfires were likely patchy but mostly high-severity, as sagebrush is easily killed by fire and even low-intensity fire can result in high mortality rates, and thus created a mosaic of community types ranging from early-successional grasslands to groves of mature shrubs and long-lived bunchgrasses and forbs (Baker 2011).

EuroAmerican settlement of the intermountain western United States brought numerous changes to natural disturbance regimes and successional processes, as a result of land use, introduction of non-native plant species, anthropogenic wildfire ignition and suppression, and replacement of native ungulates with livestock. Altered successional trajectories in areas historically occupied by sagebrush ecosystems are evinced by recent expansion of juniper/pinyon woodlands in some upland areas, and extensive invasion of annual weed communities in many mid- to low-elevation areas. Since their introduction in the late 19th century, cheatgrass (*Bromus tectorum*), medusahead (*Taeniatherum caput-medusae*), and other Eurasian grasses and forbs have replaced or severely invaded half or more of the historical sagebrush plant communities in the Great and Columbia Basins

(Knick et al. 2004). This major degradation threat largely motivates the following research.

Chapter 2: Use of Terrestrial Laser Scanning to Model Fuel Characteristics in Shrub-Steppe

Abstract

Invasion by non-native plants, climate change, and other factors are altering ecosystem processes in sagebrush steppe shrublands of the western U.S., with notable effects on vegetation composition, fuels structure, and fire regimes. In particularly arid regions, wildfires are contributing to a conversion of native shrublands to communities dominated by fire-prone invasives via a positive feedback loop, which can result in long-term degradation of burned areas. Efficient methods of vegetation inventory over large areas, such as remote sensing, are essential to understand and manage changes in vegetation conditions and to anticipate future wildfires. However, the application of information collected from aerial or satellite platforms to shrub-steppe ecosystems at a local scale is limited by spectral signal mixing and coarseness of data relative to low-stature vegetation. Terrestrial laser scanning (TLS) technology provides rapid collection of high-resolution structural information at ranges up to hundreds of meters, offering an opportunity to efficiently record vegetation characteristics in large swaths. We tested the ability of TLS-derived indices to predict biomass and canopy cover of several vegetation classes in shrub-steppe plots in southwestern Idaho, using data collected at 1 m quadrats to train models constructed using the Random Forests algorithm. We show that TLS window statistics of point geometry can be used to predict canopy cover fraction of annual grasses, perennial grasses, forbs, bare earth/litter, and shrubs, and biomass of herbaceous vegetation and shrubs, with models varying in strength between $R^2 = 0.28$ and $R^2 = 0.72$.

2.1. Introduction

The sagebrush steppe biome occupies 47 million ha of semiarid rangelands in the western United States (Bukowski and Baker 2013) and is in rapid decline. Within the upper Snake River sub basin, Idaho, sagebrush steppe ecosystems presently cover less than 58% of their historical range (NPCC 2004). While conversion to agriculture and urban development accounts for a portion of this loss, the majority is due to altered regimes of succession resulting from invasion by non-native grasses and forbs. In a phenomenon known as the “grass-fire cycle” (D'Antonio and Vitousek 1992, Knick et al. 2004), the presence of cheatgrass (*Bromus tectorum*), medusahead (*Taeniatherum caput-medusae*), and other alien annual plants adds fine dry biomass to shrubland fuelbeds, with the effect of increasing the rate and severity of wildfire events. After burns, these invasives rapidly fill cleared areas, outcompeting native plants for water and space. After several cycles of progressively larger proportions of alien annuals promoting progressively more frequent and severe wildfires, the plant community is reduced to a steady state of pyric annual grassland (Balch et al. 2013, Knick 1999). Deleterious consequences of this shift include increased wildfire hazard, decreased soil retention, decreased grazing productivity, and loss of biodiversity (Brooks et al. 2004, D’Antonio and Vitousek 1992, Sankey et al. 2012).

How best to manage and mitigate the degradation of sagebrush-dominated rangelands is a topic of ongoing research (e.g. Shinneman et al. 2011). Towards this, efficient and accurate methods to inventory vegetation in rangeland ecosystems are needed to collect baseline information about plant community characteristics, evaluate wildfire risk, and assess the impact of landscape treatment efforts. Historical efforts to take stock of rangeland vegetation have relied on hand-measured metrics, such as transect and frame-based measurements in plot-scale studies (Davies et al. 2012), and harvested dry weight and various volume derivations for studies at the scale of individual plants (Uresk et al. 1977). These manual methods are accurate, but limited in scope by manpower and logistics.

Remote sensing technology offers the ability to extend measurements of vegetation traits across the vast and often-remote rangeland landscapes of the western United States. However, the small stature, mute color, and sparse canopies of individual plants, and their sparse arrangement across the landscape, poses challenges to interpretation of spectral data, and efforts to apply spectral remote sensing to shrub-steppe inventory have been limited to qualitative mapping of broad ecosystem types (Jacobson and Synder 2000, Knick et al. 1997, Okin et al. 2001). Similarly, the utility of remote sensing via aerial laser scanning is limited by the low point density and high error of typical collections, relative to low-stature rangeland vegetation (Mitchell et al. 2011, Streutker and Glenn 2006).

Allowing structural measurements at centimeter resolution at ranges extending to hundreds of meters, terrestrial laser scanning (TLS) provides an intermediate approach between highly-localized, precise field measurements and spatially-extensive, relatively-coarse remotely-sensed measurements from aerial and satellite platforms. A notable disadvantage of TLS sampling is that collections are prone to occlusion, where areas lying behind protrusions (e.g. shrubs) are blocked from the sensor's line-of-sight. This problem can be partially mitigated by scanning an area from several different angles.

Past work has used TLS to predict biomass of individual sagebrush shrubs (Olsoy et al. 2014a,b) and predict the height and crown area of individual shrubs across large plots (Vierling et al. 2013). In this study, we used local measures of TLS point cloud geometry to model biomass and canopy cover of several rangeland vegetation types, using field measurements for training and validation. We demonstrate the ability of TLS imagery to predict vegetation characteristics across large plots without explicitly classifying or delineating individual plants.

Models were derived using Random Forests regression analysis. Often applied to "wide" datasets where the number of predictor variables approaches or exceeds the number of measurements, the Random Forests algorithm employs a multitude of decision trees to model the most likely response to each combination of predictor variables (Breiman 2001). Instead of calculating true R^2 and RMSE values, for each tree the algorithm splits data into training and testing datasets, measuring model performance in each tree as fit to 37% data retained as an "out-of-bag" testing datasets preventing problems of over-fitting (Breiman 1996). Previous work has applied Random Forests to model vegetation structure using window measurements of LiDAR point cloud geometry (Hudak et al. 2008, Mitchell et al., in review), although we are not aware of any work using the algorithm to make predictions based on TLS point clouds. Random Forests creates models which often maximize predictive power, but these models are "black boxes" where the mechanism of relationships is explicitly unknown. The algorithm was well-suited to this study as both our predictor and training data proved complex and without intuitive correlations, and because we prioritize predictive power over clearly-defined mechanisms of relationships.

2.2. Methods

Study area

The study area is located within the Morley Nelson Snake River Birds of Prey National Conservation Area (NCA), which encompasses 242,773 ha of the Snake River Plain ecoregion in southeastern Idaho, USA (**Figure 2.1**). In an average year, the NCA receives 20 cm of precipitation, 74 days with a high temperature greater than 32° C, and 98 days with a low temperature below 0° C (WRCC, 2012). Surface geology consists mainly of plateaus and rolling uplands of windblown soils, interspersed by basalt outcrops.

The native flora assemblage is composed of an understory of biological crusts and sparse native bunchgrasses, overlain by an open canopy of shrubs ranging up to 2 m tall. While big sagebrush (*Artemisia tridentata*) is dominant regionally, numerous other shrub species contribute diversity and may be individually most common at the site level.

Although wildfire events are historically rare in the NCA, over half of the area has burned since 1980. The resulting landscape is a mosaic of plant communities, with compositions spanning a gradient between intact native shrublands, shrublands degraded by biological invasion and wildfire, and grasslands where native plants have been fully replaced by cheatgrass and other invasive annuals. Currently 37% or less of the NCA retains an intact native shrubland community. Active management on the NCA to promote native vegetation and reduce wildfire hazard includes strategic grazing, mechanical planting of native species, and mowing (USDI BLM 2008).

Data Collection

Square plots (n = 26, 1 ha in area) for manual and TLS sampling were established at locations throughout the western NCA, using a stratified random sampling approach. The sites were selected to capture a variety of plant community compositions and for accessibility. In the center of each plot, a 3 x 3 grid of 1 m^2 quadrats was established, with 25 m spacing between adjacent quadrats. Over the 26 plots, a total of 234 quadrats were established.

The corners of each plot were precisely located using a survey-grade GNSS receiver, and elevated reflector discs were deployed at each corner to provide control points for coregistration and georegistration of TLS scans. A small, elevated reflector was placed at the center point of each quadrat as a marker to facilitate precise location in the TLS point cloud.

TLS collection was performed using a Riegl VZ-1000 near-infrared scanner mounted on a 2 m tripod. At a range of 100 m, this instrument has a reported accuracy of $\sigma = 8$ mm and a beam divergence of 30 mm (Riegl, Austria). Single-return scans were performed with 0.02 degrees of separation between pulses. Plots were scanned from five positions, once from the approximate midpoint of each side and once from the approximate plot center. Slight leeway in scanner location selection allowed for adaptation to reduce occlusion in each scan.

A nadir photograph was collected from 1.5 m above each quadrat, imaging an area approximately 1 x 1.5 m. Photographs were classified by species at 100 gridded points, providing an estimate of quadrat canopy composition. This information was aggregated to estimate canopy cover of the following classes: bare earth/litter, annual grasses, perennial grasses, forbs, and shrubs. Aboveground vegetation within the quadrat was then harvested and categorized as shrub or herbaceous. Where shrubs were too bulky to be harvested efficiently, a portion was collected for reference, and the number of equivalent portions remaining in the quadrat was estimated. Harvested vegetation was kiln-dried before weights by class were recorded. All manual sampling was performed by staff of the USGS Forests and Range Ecosystem Science Center, in Boise ID (Shinneman et al. 2011). These canopy cover and biomass data were used to train and validate interpretation of TLS datasets.

Figure 2.1. The study area located in southwest Idaho, USA. The Morley Nelson Snake River Birds of Prey National Conservation Area is outlined in red, and research plots (n = 26) are show as black stars.

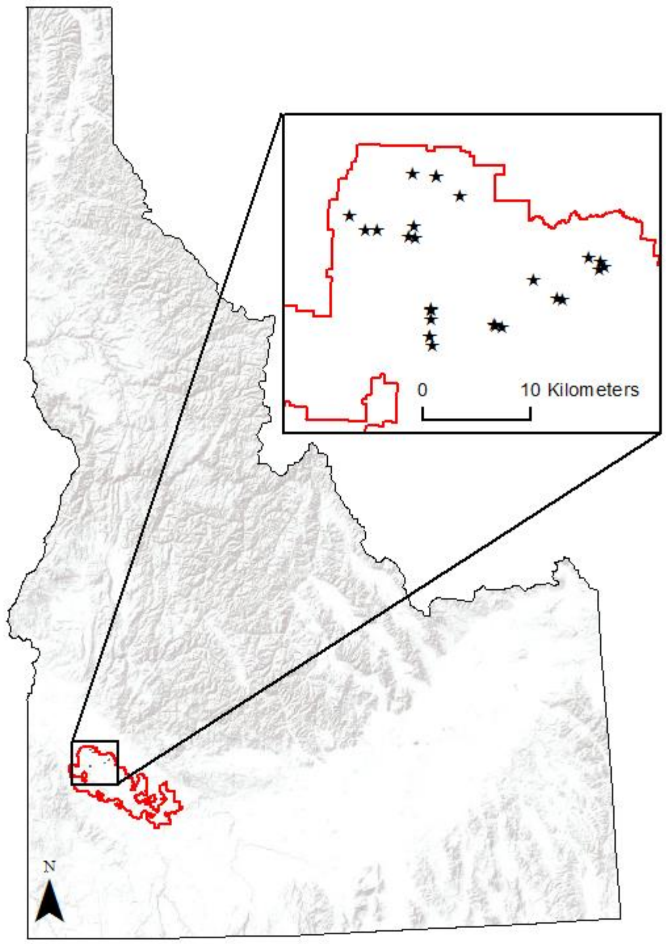

All TLS sampling was performed between May 15 and June 14, 2013. By this date grasses and forbs were mostly senescent, but structurally intact. Manual sampling was carried out an average of 10 days after TLS sampling, with the exception of 6 plots which were manually sampled between 136 and 142 days later (**Table A.3)**.

Table 2.1. Window statistical descriptors calculated about TLS point distribution. The minimum, maximum, standard deviation, range, and mean of each descriptor within the bounds of each quadrat were used as predictor variables of each feature.

Statistic
5th percentile height
10th percentile height
25th percentile height
50th percentile height
75th percentile height
90th percentile height
95th percentile height
Canopy relief ratio
Coefficient of variation of heights
Count of all returns
Count of ground returns
Count of vegetation returns
Interquartile range of heights
Kurtosis of heights
Maximum height
Mean absolute deviation from mean height (AAD)
Mean of heights
Median absolute deviation from median height (MAD)
Minimum height
Percent of area covered by vegetation
Percent of heights between 0 and 1 m tall
Percent of heights between 1 and 2.5 m tall
Percent of returns modeled as ground
Range of heights
Skewness of heights
Standard deviation of heights
Texture of heights (standard deviation of heights between 5 cm and 15 cm)
Total vegetation density (((count of vegetation points)/(count of ground points))*100)
Variance of heights

Processing

TLS point clouds were subsampled to a minimum spacing of 1 cm between points. Any spurious points, and points representing the quadrat marker reflector, were manually removed. Using the BCAL LiDAR Tools software (http://bcal.boisestate.edu/tools/lidar), ground filtering was performed and point clouds were converted to multiband rasters with pixel sizes 5 cm, 10 cm, and 20 cm. Raster values were calculated as a suite of 29 statistical descriptors of TLS point distribution within the window of each pixel (**Table 2.1**). The mean, minimum, maximum, range, and standard deviation of all pixel-wise descriptors within each quadrat were recorded.

Quality control

The portion of TLS point clouds within the bounds of each quadrat was visually inspected and assessed for further processing. Quadrats were assigned a qualitative score of 1 (lowest quality) to 3 (highest quality) based on the number and spread of points modeled as ground within a plot (**Figure 2.2**). Quadrats scoring “1” contain no ground points, quadrats scoring “3” contain several ground points in each quadrant, while quadrats scoring “2” contain ground points which are few or are not distributed throughout the quadrat. This scoring method was chosen firstly because an insufficient distribution of ground points may cause erroneous modeling of vegetation height values, and secondly because the frequency and spread of ground points is a simple way of quantifying the extent of areas in a quadrat that were occluded from sampling. Additionally, quadrats where overall sampling coverage was exceptionally poor (the entire quadrat was in essence unsampled) were flagged and discarded.

Figure 2.2. Examples of TLS point cloud in quadrats assigned to each score. Vegetation points are shown in green and ground points are shown in brown. The boxes around points show the extent of the quadrat—heights vary but each box has a 1 x 1 m base.

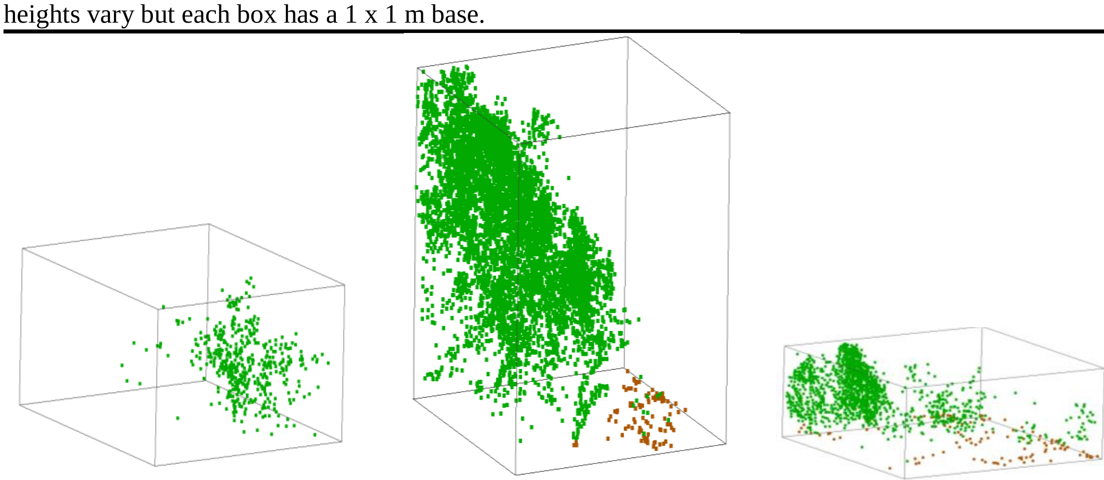

Score 1 | Score 2 | Score 3

Random Forests Modeling

Random Forests regression (Salford Predictive Modeler Software Suite version 7, Salford Systems, San Diego, CA) was applied to derive a model predicting field-measured vegetation characteristics using the mean, minimum, maximum, range, and standard deviation of TLS window statistics as predictor variables (e.g. the standard deviation of 10^{th} percentile height values of all pixels in a quadrat), producing 145 predictor variables in total. The bulk of these predictors were of low influence in Random Forests models, and the inclusion of most actually decreased model performance in the testing dataset. Optimal models were derived experimentally by iteratively removing lowest-influence predictor variables until this method decreased model R^2. Each combination of the remaining predictor variables was tested, and the model was selected which minimized the number of predictor variables while retaining high R^2 and low RMSE. Where significant trade-offs were presented in measurements of model strength, the rationale was used that model accuracy (R^2) was more important than model precision (RMSE), and both were more important than model parsimony (number of predictor variables). Random Forests regression analysis was performed using each combination of window size and quality score.

To validate the assumption that data from each quadrat could be considered an independent sample (uncorrelated by plot), the residuals of each model were examined for each plot's data. We found that for each model, the residuals of modeled values from each plot appeared to be randomly distributed around 0, indicating that the relationship between manually-sampled values and TLS sampling does not change between plots (**Figure A.1**).

2.3. Results

Field-measured values of biomass and fractional canopy cover were highly non-normal, with most biomass and cover estimates clustering near the low and high ranges of measurements. Likewise, the standard deviation of measurements approached or exceeded the mean measurement of each variable (**Table 2.2**).

Table 2.2. Statistics describing the manual measurements of each predicted feature (n = 206). Minimum values were all 0.

Feature	25^{th} percentile	Median	75^{th} percentile	Max	Mean	SD
Shrub cover (%)	0.0	0.0	8.2	60.8	7.5	13.7
Bare earth/litter cover (%)	13.1	43.1	61.4	94.0	40.8	27.1
Annual grass cover (%)	0.0	13.0	73.3	100.0	34.5	38.0
Perennial grass cover (%)	1	7.0	21.0	70	13.4	15.3
Forb cover (%)	0.0	0.0	3.0	68	3.9	8.8
Shrub biomass (g)	0.0	0.0	18.2	2476	106.2	321.6
Herbaceous biomass (g)	56.6	97.1	179.8	1193.1	146.2	157.9

Of the 234 quadrats collected, 28 were discarded due either to occlusion (poor sampling coverage) or obvious and irreparable locational errors in manually-sampled data. Of the 206 remaining, 9 were assigned a score of 1, 98 were assigned a score 2, and 99 received a score of 3 (**Table A.2**). In spite of the large number of quadrats judged to be sampled suboptimally, the effect of limiting analysis to only high-scoring quadrats on model goodness-of-fit was not major (difference in $R^2 < 0.2$ and generally near $R^2 = 0$, in some cases shrinking the pool of data actually caused R^2 to decrease) (**Table A.1**). In the interest of demonstrating the resilience of this approach to suboptimal sampling, results are reported for models using the entire population of quadrats (except the 28 discards, remaining n = 206) for training and validation.

The pixel size (the window in which point cloud statistics were calculated) yielding the best model varied among the measurement being predicted. Descriptors calculated using a 5 cm pixel size yielded the strongest predictors for shrub cover (R^2 = 0.72, RMSE = 7.3%), annual grass cover (R^2 = 0.61, RMSE = 23.7%), and forb cover (R^2 = 0.53, RMSE = 6.1%). A 10 cm pixel size yielded the strongest predictors of perennial grass cover (R^2 = 0.28, RMSE = 12.9%), bare earth/litter cover (R^2 = 0.40, RMSE = 20.9%), and shrub biomass (R^2 = 0.64, RMSE = 191.7 g), and a 20 cm pixel size yielded the strongest predictors of herbaceous biomass (R^2 = 0.55, RMSE= 106.5 g).

All predictive models yielded by the Random Forests algorithm achieved maximum goodness-of-fit using 4 or fewer predictor variables. While the combination of predictors used is inconsistent among models, some predictors (e.g. maximum of 50th percentile heights) are used more commonly than others. The predictors and pixel sizes used and measures of strength are recorded in **Table 2.3**.

2.4. Discussion

Using contemporaneous collection of TLS and manually-sampled datasets, this study demonstrated the potential of TLS to predict canopy cover and biomass of several vegetation classes at the 1 m scale, across large plots. With these methods TLS collections may be used as a powerful complement to manual sampling, by using localized measurements to train models of vegetation characteristics across broad, contiguous areas. These results extend the known capabilities of TLS collections in sagebrush-steppe ecosystems, which have previously been demonstrated to enable detection and prediction of height and crown area (Vierling et al. 2013), and precise biomass prediction (Olsoy et al. 2014a,b), of individual sagebrush shrubs.

Generally, the accuracy of our models was high, as indicated by R^2 values above 0.5. However, precision was low, as indicated by RMSE values ranging between 55%

and 195% of mean manual measurements. Considering numerous likely sources of error (discussed below) in our methodology, it is unsurprising that model predictions are rough. Future studies which duplicate our methods may accommodate accurate but imprecise modeling of features by treating predictions as categorical, thus generalizing them. It is also likely that future studies could improve model precision by collecting finer scale manual measurements for training and validation, and by removing some of the errors in sampling that we encountered.

Table 2.3. Strength, pixel size used to calculate point cloud geometry, and predictors listed by relative importance of the selected Random Forests models (n = 206).

Feature	Pixel size	Predictors	R^2	RMSE
Annual grass cover	5 cm	1. Maximum of 50th percentile heights 2. Standard deviation of minimum heights 3. Mean of 50th percentile heights	0.61	23.7%
Bare earth/litter cover	10 cm	1. Maximum of 50th percentile heights 2. Mean of % of heights between 0 and 1m 3. Mean of 50th percentile heights	0.40	20.9%
Forb cover	5 cm	1. Mean of 50th percentile heights 2. Maximum of 50th percentile heights 3. Minimum of 50th percentile heights 4. Mean of kurtosis of heights	0.53	6.1%
Perennial grass cover	10 cm	1. Maximum of 50th percentile heights 2. Minimum of coefficient of variation of heights 3. Mean of absolute deviations from median height 4. Maximum of minimum heights	0.28	12.9%
Shrub cover	5 cm	1. Standard deviation of maximum heights 2. Standard deviation of 75th percentile heights 3. Maximum of maximum heights 4. Maximum of 50th percentile heights	0.72	7.3%
Herbaceous biomass	20 cm	1. Mean of % of returns modeled as ground 2. Range of 5th percentile heights 3. Mean of minimum heights 4. Maximum of 50th percentile heights	0.55	106.3 g
Shrub biomass	10 cm	1. Mean of count of vegetation returns 2. Mean of mean heights 3. Mean of absolute deviations from median height 4. Mean of % of returns modeled as ground	0.64	191.7 g

Two predictive models, those of perennial grass cover and bare earth/litter cover, substantially underperformed the others. In the case of perennial grass cover, we think that consistent identification was likely challenged by the diverse sizes of perennial grasses, which varied greatly depending on species and site. In particular, there is little structural difference between small perennial grasses (e.g. short specimens of sandberg's bluegrass, *Poa secunda*) and annual grasses such as cheatgrass. Meanwhile, though the distinct flatness of the bare/earth litter class suggests that it would be easily classified apart from vegetation cover classes, as the lowest-lying class it was also the most likely to be unsampled due to occlusion. Since our calculation of quadrat-wise statistics excluded occluded pixels from consideration, it is probable that the signal of bare earth/litter was often simply lost.

Successfully applying grid-based statistical metrics of TLS-derived shrub height and geometry to model class-wise canopy cover and biomass demonstrates that vegetation characteristics may be predicted using remotely-sensed datasets without explicit classification and delineation of plants. This capability is especially valuable when complementary manual sampling is performed on a per-area, rather than per-plant basis, as was the case in this study. Additionally, Vierling et al. (2013) noted that automated detection and delineation of sagebrush shrubs <1.5 m diameter using TLS point clouds was challenging, which suggests that window-based approaches may be most effective to predict characteristics of small-stature rangeland plants.

Predicting canopy cover and biomass without attempting to delineate individual plants offers some disadvantages. Allometric relationships between plant geometry and biomass would be expected to be strongest when a single, complete plant is considered. By contrast, data collected in this study may consider only portions of plants, and group several plants and even several plant types together into a measurement. For example, entire shrubs and single shrub boughs have different relationships between bulk structural geometry and biomass because single boughs do not contain large and weighty trunks. In the common instance where a quadrat containing annual grasses was overhung by a shrub bough, a correct model of class-wise biomass needed to account for not only the presence of two classes of vegetation, but also the particular relationship of geometry to biomass for the pertinent portion of a shrub. For a model based on statistics that describe TLS point cloud geometry within the quadrat as a whole, this is a challenging task. Likewise, not explicitly classifying vegetation types adds to potential confusion in modeled values where different vegetation types exhibit similar measurements of geometry after values are aggregated for entire quadrats. For example, several tall, narrow, individual bunchgrasses may exhibit measurements of geometry resembling those of a single large and wide shrub, when data from throughout the quadrat is aggregated into a single value. These factors may partly explain the lower strength of our models compared to estimates of shrub biomass (or volume, a precise proxy) in studies focused on individual plants (e.g. Kaluza et al. 2012, Loudermilk et al. 2009, Olsoy et al 2014a,b).

The collaborative collection of field data introduced idiosyncrasies to our datasets, which may contribute substantially to model error. Estimates of class canopy cover were derived from photographs 1 x 1.5 m in extent, rather than the 1 x 1 m extent of quadrats, and because photos were not oriented consistently it was not possible to adjust the considered portion of TLS point clouds to correspond with the extent of the photo. Small errors of rotation and translation in harvest quadrat placement may introduce substantial errors to our analysis where a large portion of the canopy cover or biomass of a vegetation class falls close to a quadrat's edge. The method of harvesting only a portion of large shrubs may also introduce substantial error in shrub biomass measurements if the collected portion is not adequately representative of the shrub as a whole, or if the number of portions remaining in the quadrat was incorrectly estimated. Although growth and decomposition of vegetation is slow in our field area, the delay between TLS and manual sampling allowed time for herbivory, wind, and other factors to alter vegetation before manual sampling was performed. Each of these sources of error could be minimized in future efforts.

A final source of error worth mentioning is the potential for confusion introduced by forbs species (e.g. tall tumble mustard, *Sisymbrium altissimum*) that have a strong structural similarity to shrubs. A disadvantage of relying exclusively on structural indices is the inability to distinguish between vegetation types with roughly the same shape. However, forbs resembling shrubs tend to be concentrated on the landscape and were common within only a few of our plots (**Table A.4**). Future studies might overcome this confusion by integrating high-resolution spectral information gathered from airborne or satellite platforms. Unfortunately, although "intensity of return" values recorded by many TLS instruments (which indicate the spectral reflectance of targets at the laser bandwidth) may be used to classify different vegetation types sampled at close ranges (Olsoy et al. 2014a,b), we found that the intensity of return yielded by a given target was not consistent at different ranges, hindering the usefulness of this data in parsing targets across large plots.

We found that the window size used to calculate TLS point cloud geometry descriptors affected the strength of models, but that no window size was consistently superior. While the mechanism driving this effect is unclear, it suggests that the ideal trade-off between fine-scale measurement of point cloud geometry and measurement resilience to fine-scale stochasticity in TLS point clouds differs depending on the characteristic being modeled. Moreover, this trade-off exists despite window measurements in each quadrat eventually being aggregated. In general it appears that 5 and 10 cm windows outperform 20 cm windows, but our analysis suggests that it is worth testing several window sizes to derive the strongest predictors of each field measurement.

Though the strength of some models did improve when considering only quadrats judged to have optimal sampling quality, we were able to derive satisfactory models predicting all field-measured features while excluding only the 28 quadrats which were almost entirely unsampled. This is remarkable considering that a minority of quadrats were judged to have been sampled optimally, and demonstrates the resilience of our window statistics-based models to both the presence of occluded regions within quadrats and small errors in modeled vegetation height arising from spotty ground-level sampling.

Although the 5-position TLS sampling methodology provided highly-redundant coverage in general, sampling occlusion was still a major challenge in this study that led to a large amount of data being discarded. Occlusion was most problematic in plots with high shrub cover, where interstitial spaces lying more than a few meters from scanning positions commonly escaped the instrument’s line-of-sight from all 5 scan positions. Consequently, only the upper canopies of tall shrubs were reliably sampled. This problem could be partially avoided by elevating the scanner far above the typical vegetation height, as done in Vierling et al. 2013, or by increasing the number of scanning positions.

In sum, we demonstrate the use of TLS to predict measurements of canopy cover and biomass of different rangeland vegetation types across 1 ha plots. These methods may improve the efficiency of ground-based vegetation inventory while providing information at superior resolution to datasets collected from airborne or satellite sensors. We show that an ensemble learning algorithm yields parsimonious and accurate models relating window statistics of TLS point cloud geometry to field-measured values, despite difficulties arising from shadowing in TLS point clouds and training and validation data that were collected at relatively coarse scales and not focused on individual plants.

The methods demonstrated here have immediate applicability to research in shrub-dominated rangelands. The ability to accurately inventory vegetation across large plots may extend the scope of current work to evaluate landscape fuel treatments, which presently rely on highly localized manual sampling measurements. Our methods as presented offer vastly increased efficiency and spatial thoroughness of vegetation inventory over traditional techniques, although at the cost of measurement precision. TLS-based models of vegetation characteristics may also serve as a stepping stone to even broader sampling methods by providing information to train interpretation of data collected from aerial or satellite platforms. Another application of spatially-explicit vegetation inventory enabled by TLS is as realistic, high-resolution input data to simulations, such as those of wildfire behavior or aeolian processes. In general, TLS collections enable creation of broad and rich models of vegetation at low logistical cost, which may aptly serve a wide variety of research and management needs.

2.5. Literature Cited

Balch, J. K., Bradley, B. A., D'Antonio, C. M., & Gómez-Dans, J. (2013). Introduced annual grass increases regional fire activity across the arid western USA (1980–2009). *Global Change Biology*, *19*(1), 173-183.

Breiman, L. (2001). Random forests. *Machine learning*, *45*(1), 5-32.

Breiman, L. (1996). Out-of-bag estimation. *Technical report 1996b*. Berkeley, CA: Statistics Department, University of California Berkeley.

Brooks, M. L., D'antonio, C. M., Richardson, D. M., Grace, J. B., Keeley, J. E., DiTomaso, J. M., Hobbs, R.J, Pellant, M., & Pyke, D. (2004). Effects of invasive alien plants on fire regimes. *BioScience*, *54*(7), 677-688.

Bukowski, B. E., & Baker, W. L. (2013). Historical fire regimes, reconstructed from land-survey data, led to complexity and fluctuation in sagebrush landscapes. *Ecological applications*, *23*(3), 546-564.

D'Antonio, C. M., & Vitousek, P. M. (1992). Biological invasions by exotic grasses, the grass/fire cycle, and global change. *Annual review of ecology and systematics*, 63-87.

Davies, K. W., Bates, J. D., & Nafus, A. M. (2012). Vegetation response to mowing dense mountain big sagebrush stands. *Rangeland Ecology & Management*, *65*(3), 268-276.

Hudak, A. T., Crookston, N. L., Evans, J. S., Hall, D. E., & Falkowski, M. J. (2008). Nearest neighbor imputation of species-level, plot-scale forest structure attributes from LiDAR data. *Remote Sensing of Environment*, *112*(5), 2232-2245.

Jacobson, J. E., & Snyder, M. C. (2000). *Shrubsteppe mapping of eastern Washington using Landsat satellite Thematic Mapper data.* Spatial Data Management Section, Science Division, Wildlife Program, WA Department of Fish and Wildlife.

Kałuża, T., Tymków, P., & Strzeliński, P. (2012). Use of remote sensing for investigating riparian shrub structures. *Polish Journal of Environmental Studies*, *21*(1).

Knick, S. T. (1999). Requiem for a sagebrush ecosystem? *Northwest Science*, *73*(1).

Knick, S. T., Rotenberry, J. T., & Zarriello, T. J. (1997). Supervised classification of Landsat Thematic Mapper imagery in a semi-arid rangeland by nonparametric discriminant analysis. *Photogrammetric Engineering and Remote Sensing*, *63*(1), 79-86.

Knick, S. T., Schroeder, M. A., & Stiver, S. J. (2004). *Conservation assessment of greater sage-grouse and sagebrush habitats.* Cheyenne, WY: Western Association of Fish and Wildlife Agencies.

Loudermilk, E. L., Hiers, J. K., O'Brien, J. J., Mitchell, R. J., Singhania, A., Fernandez, J. C., Cropper, W.P. & Slatton, K. C. (2009). Ground-based LIDAR: a novel approach to quantify fine-scale fuelbed characteristics. *International Journal of Wildland Fire*, *18*(6), 676-685.

Mitchell, J. J., Glenn, N. F., Sankey, T. T., Derryberry, D. R., Anderson, M. O., & Hruska, R. C. (2011). Small-footprint LiDAR estimations of sagebrush canopy characteristics. *Photogrammetric Engineering & Remote Sensing*, *77*(5), 521-530.

Mitchell, J.J., Shrestha, R., Spaete, L.P., Glenn, N.F. (2014). Combining airborne LiDAR and hyperspectral data across local sites for upscaling shrubland structural information: lessons for HyspIRI. *Remote Sensing of Environment* (in review).

Northwest Power and Conservation Council. (2004). *Upper Snake subbasin assessment*. Portland, OR: Northwest Power and Conservation Council.

Okin, G. S., Roberts, D. A., Murray, B., & Okin, W. J. (2001). Practical limits on hyperspectral vegetation discrimination in arid and semiarid environments. *Remote Sensing of Environment*, *77*(2), 212-225.

Olsoy, P, N Glenn, & Clark, P. (2014). Estimating sagebrush biomass using terrestrial laser scanning (TLS). *Rangeland Ecology & Management*, *67* (2): 224-228.

Olsoy, P. J., Glenn, N. F., Clark, P. E., & Derryberry, D. R. (2014). Aboveground total and green biomass of dryland shrub derived from terrestrial laser scanning. *ISPRS Journal of Photogrammetry and Remote Sensing*, *88*, 166-173.

Sankey, J. B., Germino, M. J., Benner, S. G., Glenn, N. F., & Hoover, A. N. (2012). Transport of biologically important nutrients by wind in an eroding cold desert. *Aeolian Research*, *7*, 17-27.

Shinneman, D., Arkle, R., Pilliod, D., Glenn, N.F. (2011). *Quantifying and Predicting Fuels and the Effects of Reduction Treatments Along Successional and Invasion Gradients in Sagebrush Habitats*.
Retrieved from:
http://www.firescience.gov/JFSP_funded_project_detail.cfm?jdbid=%24%26ZO9V0%20%20%0A

Streutker, D. R., & Glenn, N. F. (2006). LiDAR measurement of sagebrush steppe vegetation heights. *Remote Sensing of Environment*, *102*(1), 135-145.

Uresk, D. W., Gilbert, R. O., & Rickard, W. H. (1977). Sampling big sagebrush for phytomass. *Journal of Range Management*, 311-314.

USDI Bureau of Land Management. (2008). *Snake River Birds of Prey National Conservation Area Proposed Resource Management Plan and Final Environmental Impact Statement, Boise, ID.*

Vierling, L. A., Xu, Y., Eitel, J. U., & Oldow, J. S. (2013). Shrub characterization using terrestrial laser scanning and implications for airborne LiDAR assessment. *Canadian Journal of Remote Sensing*, *38*(6), 709-722.

Western Region Climate Center. (2012). *Swan Falls Power House*, *Idaho*, *Period of Record General Climate Summary*.
Retrieved from: http://www.wrcc.dri.edu/cgi-bin/cliMAIN.pl?id8928

Chapter 3. Methodological Considerations of Terrestrial Laser Scanning in Rangelands

Abstract

Terrestrial laser scanning (TLS) provides fast collection of high-definition structural information, making it a valuable field instrument to many natural science disciplines. A weakness of TLS collections is the issue of “shadowing”, unsampled regions that occur in point clouds where the sensor’s line-of-sight is occluded during sampling. This problem may be mitigated by scanning target areas from several positions, increasing the chance that any given area will fall within the scanner’s line-of-sight from at least one position. Although many studies employ this method, most only incidentally describe shadowing problems and methods used to resolve them. Because TLS collections are often employed in remote regions where the scope of sampling is limited by logistical factors such as time and battery power, field protocols which maximize efficiency may increase the quantity and quality of data collected. This study aims to inform researchers seeking to optimize TLS methods in rangeland ecosystems through three analyses: First, we quantify the 2D extent of shadowed regions as an effect of range from scanning position. Second, we measure the efficacy of additional scanning positions on the reduction of 2D shadowed regions using progressive configurations of scan positions in hectare plots. Third, we test the reproducibility of 3D sampling yielded by a 5 scan per hectare sampling methodology using redundant sets of scans. Analyses were performed using measurements at several scales, and considered plots in grass-dominated and shrub-dominated communities separately. Future studies applying TLS in similar environments may use our results as a guide to efficiently achieve predetermined standards of sampling coverage and reproducibility in datasets.

3.1. Introduction

Laser scanning, commonly called light detection and ranging (LiDAR), refers to technologies using laser pulse ranging measurements to record precise structural information about targets. Three dimensional point clouds yielded by laser scanners have proven valuable to natural sciences, particularly for broad-scale measurements of vegetation and topography. While most LiDAR datasets used in natural science research thus far were collected aerially, recent improvements in technology have led to expanded use of terrestrial laser scanning (TLS) instruments. Ground-based sampling offers several unique advantages, including ultra-high data resolution, below-canopy sampling, and low cost of collection (Heritage and Large 2009). The rapidly-growing body of work using TLS in field studies includes measurements of fine-scale geomorphology (Brodu and Lague et al. 2012), and inventory of forests (Strahler et al. 2008), shrublands (Vierling et al. 2013), and low-lying vegetation (Loudermilk et al. 2009).

A notable disadvantage of scanning from the ground is the issue of occlusion (shadowing) in point clouds, where the scanner's line-of-sight to a region is blocked by intervening objects. In aerial collections, a narrow scan angle and field-of-view cause the effects of occlusion to be highly regular, so that sampling is limited to topmost surfaces but 2D spatial coverage is largely unaffected. In TLS collections however, mainly-lateral scanning orientation may leave large data gaps where extended regions are shadowed by protruding vegetation or topographic features. These data gaps often cause TLS point clouds to be highly irregular, with regions with good sampling coverage falling immediately adjacent to regions that are unsampled entirely. Some aerial and terrestrial instruments enable partial mitigation of shadowing through detection of multiple returns of light from each pulse, allowing for sampling of several in-line targets when the first target intercepts only a portion of a pulse's footprint. However, these secondary measurements are at increased risk of "zig-zag" pulse paths that reflect off several surfaces and other complications which reduce positional certainty (Shan and Toth 2008).

Some studies have accounted for shadowing in TLS datasets by modeling unsampled features based on features which are sampled. For example, Stahler et al. (2008) infer the number of fully-occluded tree stems based on the width and density of stems that are sampled, and Henning and Radtke (2006) model plant area index in volumetric regions of canopy based on the ratio of reflection to pass-through of pulses incident to each region, rather than simply measuring the plant area that is actually sampled.

Several methodological techniques have been shown to reduce shadowed areas in TLS collections. Some improvement in sampling coverage may be effected by elevating the instrument well above the objects in the target region, which causes shadows to fall beneath protrusions rather than stretching out laterally from them. This has been done using both topographically elevated scanning position sites (Vierling et al. 2013) and elevated scanning platforms (Loudermilk et al. 2009). The most common practice may be to combine scans collected at several positions, increasing the likelihood that a region will fall in the scanner's field-of-view from at least one position. This technique may be implemented using either a standardized layout of scanning positions or one that is adaptive to local features, and has proven useful in both studies sampling extensive plots and ones focusing on individual target plants (Clawges et al. 2007, Seidel et al. 2012). A similar technique is the fusion of aerial and TLS point clouds, providing complementary sampling from both above and below forest canopies (Chasmer et al. 2004, Murgoitio et al. 2014).

Although many studies employ methods to overcome shadowing problems in TLS collections, published research that quantifies the efficacy of these techniques is scarce. A small body of literature does exist which evaluates the errors in TLS-derived elevation models caused by low vegetation occluding the ground surface (e.g. Coveney and Fotheringham 2011, Fan et al. 2014). The only work we are aware of which explicitly studies the extent of unsampled regions as a consequence of occlusion is Van der Zande et al. (2008), which evaluates the efficacy of two scanning position arrangements ("diamond" and "corners") against a single scanning position and each other at reducing shadowing in simulated forest plots. They found that both arrangements of positions outperformed sampling from a single position, even when the single scan was of much higher sampling density, but that neither arrangement yielded consistently superior results to the other.

Terrestrial laser scanning may be increasingly important as a research tool in shrublands and grasslands (e.g. Olsoy et al. 2014, Vierling et al. 2013), and its use in remote field sites is challenged by logistical concerns including time and battery power. Information about the limitations of TLS sampling may improve the efficiency of field campaigns by preventing over- or under-expenditure of effort given sampling goals.

The objective of this study is to test the extent of TLS shadowing in rangeland ecosystems and the efficacy of methods to mitigate shadowing given the common instrumentation of a laterally-scanning instrument mounted on a 2 m base. Towards this, we designed three experiments testing: 1) the effect of range-from-scanner on the extent of shadowed regions; 2) the effectiveness of multiple scanning positions at reducing total shadowed area in 1 ha plots; 3) the reproducibility of datasets yielded by a methodology employing 5 scans per hectare. All results are stratified by vegetation type, either dominantly grassland or shrubland, and several scales of measurement.

3.2. Methods

Study area

The study area is located in the Morley Nelson Snake River Birds of Prey National Conservation Area (NCA), which encompasses 242,773 ha of the Snake River Plain ecoregion in southeastern Idaho, USA (**Figure 2.1**). In an average year, the NCA receives 20 cm of precipitation, 74 days with a high temperature greater than 32° C, and 98 days with a low temperature below 0° C (WRCC, 2012). Surface geology consists mainly of plateaus and rolling uplands of loess windblown soils, interspersed by basalt outcrops. In some areas, microtopographic texture is added by pits and mounds caused by burrowing animals.

The native vegetation assemblage is composed of an understory of biological crusts and sparse native bunchgrasses, overlain by an open canopy of shrubs ranging up to 1.5 m tall. Big sagebrush (*Artemisia tridentata*) is dominant regionally, and numerous other shrub species contribute diversity and may be dominant at the site level.

Although wildfire events are historically rare in the NCA, over half has burned since 1980. The resulting landscape is a mosaic of plant communities, with compositions spanning a gradient between intact native shrublands, shrublands degraded by biological invasion and wildfire, and grasslands where native plants have been fully replaced by cheatgrass (*Bromus tectorum*) and other invasive annuals. Currently 37% or less of the

NCA retains an intact native shrubland community. Active management on the NCA to promote native flora and reduce wildfire hazard includes strategic grazing, mechanical planting of native species, and mowing (USDI 2008).

Data Collection

Plots (n = 26, 1 ha in area) for field and TLS sampling were established at locations scattered throughout the NCA, with sites divided evenly between intact or semi-intact shrublands and invasive weed communities. The corners of each plot were precisely located using a survey-grade GNSS receiver, and elevated reflector discs were deployed at each corner to provide control points for coregistration and georegistration of scans.

The collection of TLS data was performed using a Riegl VZ-1000 near-infrared (1550 nm) scanner mounted on a 2 m tripod. At a range of 100 m, this instrument has a reported accuracy of σ = 8 mm and a beam divergence of 30 mm (Riegl, Austria). Single-return scans were performed with 0.02 degrees of separation between pulses. Plots were scanned from five positions, once from the approximate midpoint of each side and once from the approximate plot center. Slight leeway (< 5 m) in scanner location selection allowed for adaptation to reduce occlusion in each scan.

Each plot was classified as "shrub" (n = 13) or "grass" (n = 13), based on the dominant community type. Proper classification was unambiguous and depended on whether the area had experienced a severe stand-replacing fire. In addition to cheatgrass and other low-lying (< 25 cm) herbaceous vegetation, grass plots sometimes contained tall bunchgrasses and structurally-sparse forbs. Vegetation in each plot was quantified manually at 9 systematically-positioned points using several methods: 1) a downwardfacing photograph was classified by landcover, allowing measurement of the unvegetated area over a 1 x 1.5 m extent; 2) the maximum height of vegetation falling in a 1 m^2 quadrat centered on each point was measured; 3) the distance in 4 cardinal directions from each point to the nearest tall bunchgrass and shrub was recorded, enabling estimation of the spatial density of individuals of both plant types where: $individuals\ per\ m^2 = \frac{1}{(mean\ of\ distances\ from\ point\ to\ stem)^2}$; 4) the canopy-spanning distance of the nearest tall bunchgrass and shrub in 4 cardinal directions from each point was measured along a line intercepting the point, allowing estimation of canopy cover fraction of both plant types assuming a circular canopy shape where: $\%\ canopy\ cover = mean((0.5 * span\ distance)^2 * \pi) * estimated\ individuals\ per\ m^2 * 0.01$. The values recorded at all 9 points were averaged for each plot, and the average and standard deviation of these plot average values are reported for all grass and shrub plots in **Table 3.1**. Elevation models of each plot derived from TLS data showed generally smooth elevation gradients of < 5%.

In 4 of the plots (shrub (n = 2) and grass (n = 2)), the scanning position layout was duplicated at a rotation of 45 degrees, yielding 2 independent sets of 5 scan positions (**Figure 3.3**). Although the square hectare plots aligned with each set of scans were rotationally offset, they shared a central 8283 m^2 region and thus we used this area for our analyses.

All TLS sampling was performed between May 15 and June 14, 2013. By this date grasses and forbs were mostly senescent, but structurally intact.

Processing

To test the effect of range on the proportion of unsampled area, the scan performed at the center of each plot was rasterized, with binary pixel values indicating the presence or absence of one or more samples measured within the pixel. The number of sampled pixels falling in 3 m intervals in range from scan position was tallied for the intervals 3 - 6 m through 96 - 99 m (**Figure 3.1**). The fraction of sampled area in each interval ring was calculated as the pixel size times the count of sampled pixels, divided by the area of the ring. This analysis was performed using 5 cm, 20 cm, and 50 cm pixels.

Table 3.1 Vegetation characteristics measured at each plot aggregated by plot type (n = 13 of each). Reported values describe per-plot measurements (e.g. "Standard deviation of unvegetated area" describes the standard deviations of per-plot estimates of unvegetated area for all grass and shrub plots, where per-plot estimates are the averages of unvegetated ground cover measurements at 9 points within the plot).

Plot type	Grass	Shrub
Average unvegetated area	19.9%	33.5%
Standard deviation of unvegetated area	13.4%	18.9%
Average maximum height	44.3 cm	56.5 cm
Standard deviation of maximum heights	7.4 cm	9.9 cm
Average spatial density of tall bunchgrasses	0.2 m^{-2}	0.1 m^{-2}
Standard deviation of spatial density of tall bunchgrasses	0.2 m^{-2}	0.1 m^{-2}
Average canopy cover of tall bunchgrasses	1.9%	0.3%
Standard deviation of canopy cover of tall bunchgrasses	2.8%	0.4%
Average spatial density of shrubs	0.1 m^{-2}	0.9 m^{-2}
Standard deviation of spatial density of shrubs	0.3 m^{-2}	0.8 m^{-2}
Average canopy cover of shrubs	1.6%	17.3%
Standard deviation of canopy cover of shrubs	3.8%	7.8%

To test the effectiveness of additional scanning positions at increasing the extent of sampling in datasets, we measured the sampled area yielded by 3 configurations of scan positions in each plot: a single center position, 3 in-line positions with 1 at the plot center and 2 on opposing edges, and 5 scans in a cross shape (**Figure 3.2**). Each of these configurations exhibits four-fold symmetry around the plot center, and are "nested" in that the 3- and 5-scan configurations consist of the next smaller configuration plus 2 new scans. The point cloud corresponding to each configuration was rasterized into binary pixels indicating presence or absence of sampling measurements, and the number of sampled pixels in the 1 ha plot was tallied for each. Since 2 arrangements of 3 in-line scan positions were possible with the available data, we used the average count of sampled pixels yielded by both. The analysis was performed for 5 cm, 20 cm, and 50 cm pixels. Additionally, this analysis was performed at the 4 plots where extra scanning was performed, allowing nested configurations of 1, 3, 5, and 9 scan positions which exhibited four-fold symmetry. Where multiple arrangements of each configuration existed, all were performed and the resultant counts of sampled pixels were averaged.

Figure 3.1. The center scan at each plot (n = 26) was divided into 3 m intervals from 3 - 6 m to 96 - 99 m from the scanner, and the proportion of sampled area in each interval was recorded. This figure shows a 1 ha shrub plot with light-colored sampled areas and black shadows, with red bands representing the boundaries between range intervals.

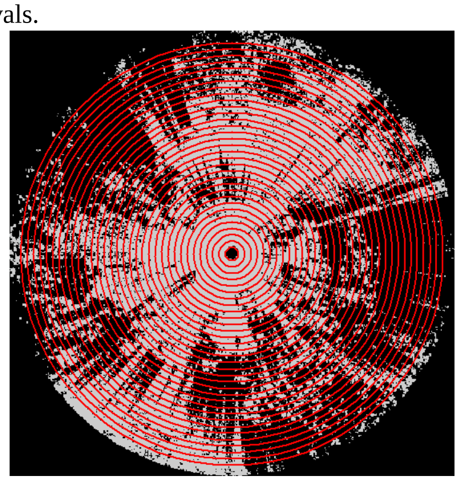

Figure 3.2. The nested scan position configurations used to study the utility of additional scanning effort. The configurations of scans including each position (configurations of 1, 3, or 5 scan positions) are indicated.

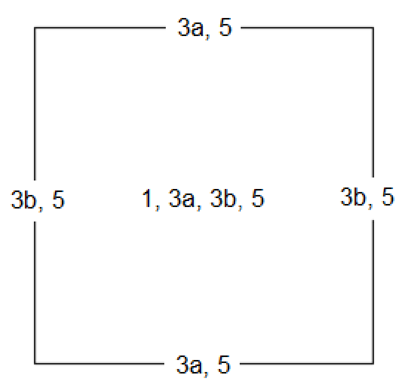

To test the reproducibility of sampling using differently-positioned implementations of a geometrically-consistent 5 scan position layout, we compared the independent point clouds yielded by the 2 sets of scans at the 4 plots where redundant sampling was performed (**Figure 3.3**). Point clouds were cropped to the 8283 m^2 region central to both sets of scans, and generalized into voxels (3D cubic regions). For each plot, a fraction was calculated where the denominator was the average number of voxels recorded in each set of scans, and the numerator was the number of voxels which were sampled commonly to both sets of scans. This indicated the fraction of data which would be sampled reliably by the scanning position layout regardless of its particular alignment relative to the plot. The analysis was performed for 5, 10, 20, and 50 cm voxels.

Figure 3.3. The redundant sampling scheme used to test repeatability of point cloud datasets yielded by a 5 scan/plot methodology (n = 4). The squares including blue and yellow regions represent differently-aligned 1 ha plots, black and grey points represent independent sets of 5 scans with theoretically-redundant sampling of the 8283 m^2 green region.

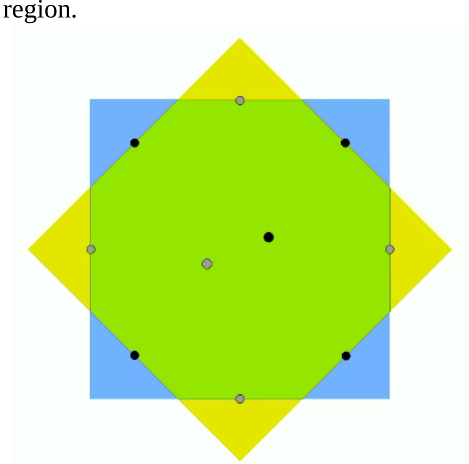

The reason for the use of different-dimension regions (2D and 3D) in the analyses was to allow consistent measurements for comparison among plots. For measurement of sampling contribution of scan positions or the effect of range on sampling coverage, the tally of sampled voxels does not yield a consistent metric because the number of voxels available to be sampled varies greatly among plots, depending on the amount of vegetation each contains. However, the number of sampled pixels is a consistent metric as each plot has the same number of pixels of any given size. In the analysis of sampling method repeatability, the varying number of occupied voxels between plots is normalized by reporting the fraction of voxels which are reproduced, a metric which will always have a value between 0 and 1.

All TLS dataset processing was performed using LasTools software (www.rapidlasso.com).

3.3. Results and Discussion

Effect of Range on Extent of Unsampled Area

Graphs showing the fractional extent of sampled area versus range from scanner are shown in **Figure 3.4**. Except at very close ranges, the average fraction of sampled pixels was lower in shrub plots than grass plots at all pixel sizes. This corresponds to expectations that the large protrusions presented by shrubs yield more extensive shadows than those produced by grass. At very long ranges, the difference between the grass and shrub plots will again approach 0 as fractional sampling coverage approaches 0, although at the ranges considered this is only demonstrated using 5 cm pixels.

A greater fraction of area is always identified as sampled as the pixel size increases. This is highly unsurprising as all areas indicating sampling presence using small presence-absence pixels will also indicate presence using larger pixels. Conversely, each large pixel indicating presence is likely to bound smaller pixels which are mixed among presence and absence.

As the pixel size used to quantify fractional sampling coverage increases, the difference in mean sampling coverage between shrub and grass plots at a given range also increases. This is likely due to different primary mechanisms of shadowing—large shadows produced by shrubs are detected using large pixel sizes, while the shadows produced by grasses are often too narrow or discontinuous to be identified using large presence-absence pixel sizes, even if these shadows are collectively spatially-extensive.

Trends of fractional sampling coverage tend to exhibit a shelf of high values (90-100%) at close ranges, with the range at which thorough sampling is determined to be achieved extending further when using larger pixel sizes and in grass plots. This shelf effect is readily accounted for by the more-acute scan angles presented at close ranges, which prevents the occurence of long lateral shadows by enabling the scanner to "see over" protruding vegetation. In grass plots, mean sampling coverage remained $\geq$ 90% up to ranges of 18 m using 5 cm pixels, 36 m using 20 cm pixels, and 66 m using 50 cm pixels. This sampling coverage among shrub plots was attained at ranges of 12 m using 5 cm pixels, 18 m using 20 cm pixels, and 30 m using 50 cm pixels. This indicates that the utility of a single scan position is substantially uncompromised by shadowing until some considerable range, depending on the scanner's height, vegetation size and density, topographic roughness, and the scale (pixel size) at which sampling coverage is quantified. A methodology using several scan positions in similar field areas could be optimized in efficiency by spacing positions at least twice the distance of the range of good performance at the scale of interest, preventing overly-redundant collection. To better identify the optimal spacing between several scan positions, further research along this line could consider the effect of range from two or more complementary positions on scanning coverage.

Beyond this shelf of high values, a negative logarithmic relationship exists between range and fractional sampling coverage. A likely mechanism of this is that a protrusion of a given size will produce more occlusion as the vector from sensor to protrusion becomes more lateral. The logarithmic trend (a steep drop-off in values which tapers as sampling coverage approaches zero) being more pronounced at smaller pixel sizes suggests that it is driven by the small shadows caused by low-lying vegetation, which are individually too small to be captured by large pixels.

A notable finding of this study is that fine and low-lying vegetation is an important mechanism of shadowing at long ranges. Although scanning was performed with a small enough angle between pulses to sample every pixel at a range of 99 m, at this range only 8% of 5 cm pixels, 37% of 20 cm pixels, and 68% of 50 cm pixels on average were sampled in grass plots. This shows that the extent of long-range sampling coverage in rangelands is controlled not by the density of sampling, but by the height and density of vegetation, topographic complexity, and the height of the scanner.

Sampling Contribution of Additional Scan Positions

Graphs showing the extent of sampled area versus the number of scan positions used are shown in **Figure 3.5**. As discussed above, the large protrusions formed by shrubs are expected to reduce measured sampling coverage by creating large shadows, and large pixels would be expected to increase measured sampling coverage by failing to identify small shadows. In line with expectations, we found that the mean area sampled in grass plots was higher than in shrub plots considering all configurations and pixel sizes, and that there was a positive effect of increasing pixel size on measured sampling coverage yielded by each scan position configuration.

Figure 3.4. The effect of range on fractional sampled area in 3 m range intervals using 5, 20, and 50 cm pixel sizes to measure sampled area. Pink lines show grass plots (n = 13) and green lines show shrub plots (n = 13), while bold and dashed lines show class means and ± 1 standard deviation, respectively.

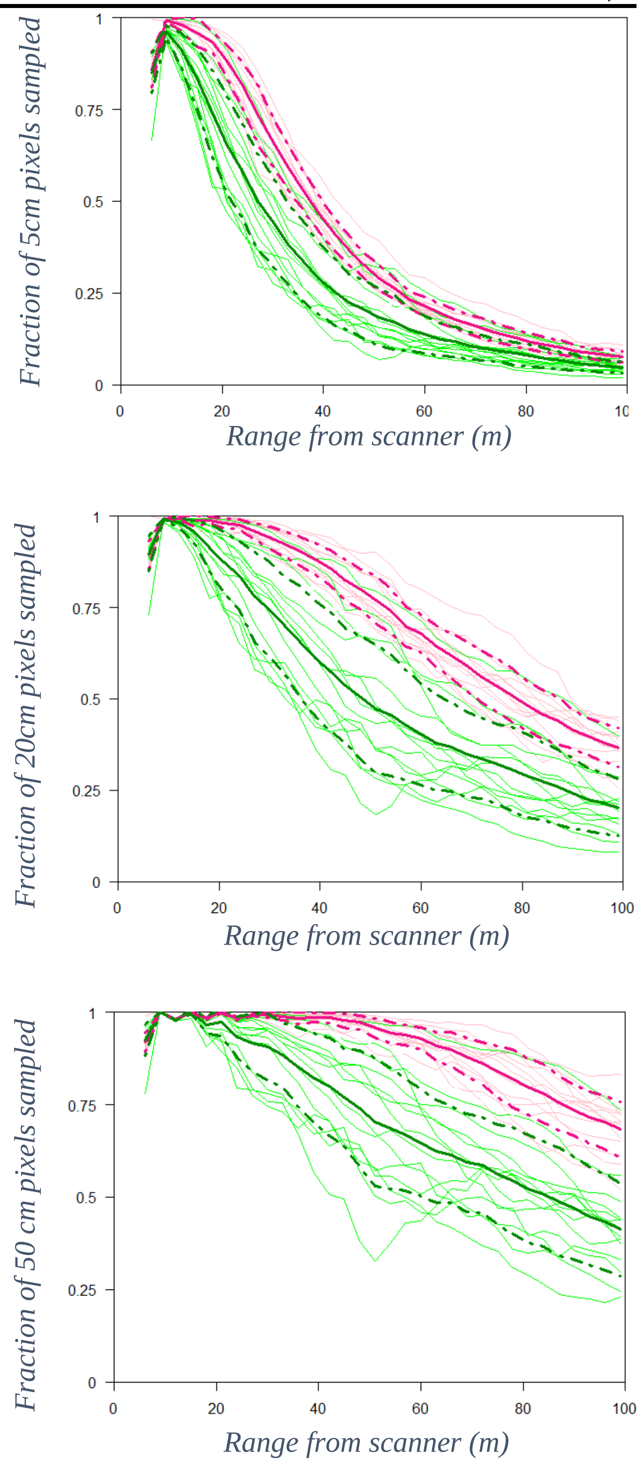

Table 3.2. The mean additional sampling coverage contributed by each configuration of additional scans, as percentage of sampled area in 1 ha plots (n = 13 each of grass and shrub plots).

Plot type	Pixel Size	1 scan coverage	3 scan coverage	5 scan coverage
Shrub	5 cm	35%	55%	69%
	20 cm	64%	82%	91%
	50 cm	83%	95%	99%
Grass	5 cm	45%	68%	82%
	20 cm	82%	95%	99%
	50 cm	96%	100%	100%

Because of the higher coverage yielded by the initial scan in grass plots and analyses using large pixel sizes, there was less room for improvement by configurations with additional scans than in shrub plots and analyses using small pixel sizes. Likewise, the contribution of data by additional scans (**Table 3.2**) consistently decreases as the number of scans already performed increases. Additional scans increased the area sampled in all cases except in grass plots using a 50 cm pixel size, where 3 scans achieved complete sampling coverage. Sampling coverage averaging 99% or 100% was also achieved in grass with 5 scans using a 20 cm pixel size, and in shrub plots with 5 scans using a 50 cm pixel size.

The 4 plots where additional sampling was performed allow further inference about cases where complete sampling coverage could not be accomplished using the 5 scan configuration. For all 4 plots (2 grass and 2 shrub), nearly-complete sampling (> 98%) was accomplished using 9 scans and a 20 cm pixel size. Using 9 scans and a 5 cm pixel size, 99% sampling coverage was accomplished for both grass plots, while shrub plots received sampling coverage of 80% and 93%. These results should be regarded as just rough estimations of typical sampling coverage yielded using 9 scan positions per plot, as they consider just 2 samples of each class. Another important note is that these statistics describe sampling coverage over a 8283 m^2 region rather than whole hectares, which not only reduces the area to be sampled but also excludes plot corners, which are the areas furthest from scanning positions.

These results provide direct guidance to maximize efficiency of TLS in grasslands or shrublands. For example, we show that a study interested in grassland features in a similar environment at the 20 cm scale needs no more than 3 scan positions per hectare to provide complete sampling coverage, while a study focused on 5 cm scale features in shrublands needs greater than 9 scan positions per hectare to achieve complete sampling coverage. A limitation of these results is that they only apply to the specific scan configurations tested, and future work would be needed to discover trade-offs between various layouts of a given number of scans.

Reproducibility of 5-Scan Position Methodology

Figure 3.6 is a graph of the fraction of volume sampled using a 5 scan position layout that was reproduced when the layout was repeated with a different alignment, versus the voxel size used for volume measurement. Voxels sampled in grass plots were reproduced more reliably than voxels sampled in shrub plots. The rates of reproducibility more closely resembled one another between the two grass plots than the two shrub plots, reflecting the greater diversity in arrangement and composition within the shrub class of plots. A qualitative examination of the shrub plot datasets showed that voxels which were not reproduced tend to represent targets below the shrub canopy, mainly ground surface or low-lying vegetation. The average percentage of voxels which occur in one set of scans and are reproduced in a second is 51% in shrub plots and 69% in

Figure 3.5. The contribution of additional scan positions to total sampled area using 5, 20, and 50 cm pixel sizes to measure sampled area. Pink lines show grass plots (n=13) and green lines show shrub plots (n = 13), while bold and dashed lines show class means and ± 1 standard deviation, respectively. At left are values calculated for all plots, and at right are values for the 2 grass plots and 2 shrub plots where additional sampling was performed.

5 scan positions	9 scan positions

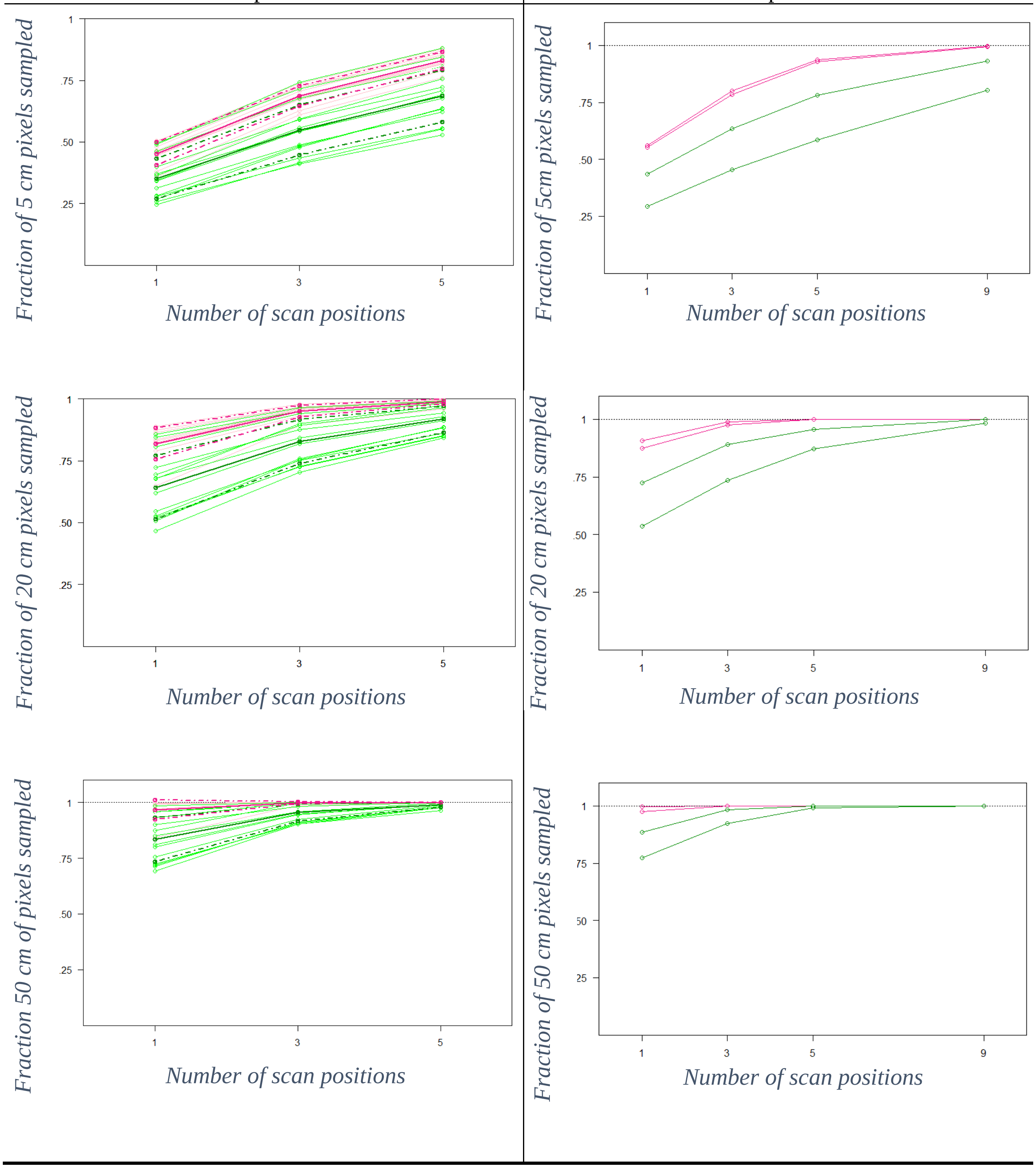

grass plots using a 5 cm voxel size, 71% in shrub plots and 87% in grass plots using a 10 cm voxel size, 84% in shrub plots and 94% in grass plots using a 20 cm voxel size, and 93% in shrub plots and 97% in grass plots using a 50 cm voxel size.

Intuitively, large voxels (coarse) were reproduced more reliably than small voxels (fine). In all cases, the positive relationship of voxel reproduction rate with voxel size tapers as voxel size increases, indicating that finer-scale discrepancies among scan sets are more prevalent than coarser-scale ones. A straightforward explanation of this is that rate of reproduction is inversely related with the amount of shadowing occurring in the point clouds of each plot, as different sets of scans may have different regions which are shadowed or sampled. In addition to inconsistently shadowed regions, fine-scale discrepancies could arise from windy conditions during scanning or small errors in coregistration of scans.

Our results indicate that about half of the data collected by a 5 scan methodology/hectare in shrub plots and two-thirds of sampled volume in grass plots is readily reproducible at 5 cm scales using the same sampling protocol, while sampling of remaining fraction is restricted to specific alignments of the scan position layout. Meanwhile, nearly all of the sampled volume in both plot types was reproduced at the 50 cm scale. While these results do not directly indicate the thoroughness of sampling or any other description of dataset quality, they may be used to infer the extent to which a quantitative analysis of TLS datasets collected using a specific protocol in rangeland ecosystems is subject to stochastic variability due to idiosyncrasies of how the scanner's field-of-view changes depending on how its specific location relates to the layout of topography and vegetation in the plot. We demonstrate clearly that studies applying TLS to detect fine scale vegetation change across large plots should take pains to use identical scanning positions at each sampling time, as using different sets of positions may indicate a substantial amount of change falsely. In change detection studies where positions are not reused exactly, our results may help to quantify error the error arising from inconsistency of scanning positions in the context of the landscape. For example, our results indicate that 2 collections using our protocol of 5 scans per hectare where scan positions were not perfectly consistent could expect about half of 5 cm voxels to be unique to each collection, even if the landscape had not actually changed in the time between collections.

Figure 3.6. The ratio of voxels that were replicated in both sets of scans to the average number of voxels recorded in 1 set of scans, considering 5, 10, 20, and 50 cm voxel sizes. Pink lines show 2 grass plots and green lines show 2 shrub plots.

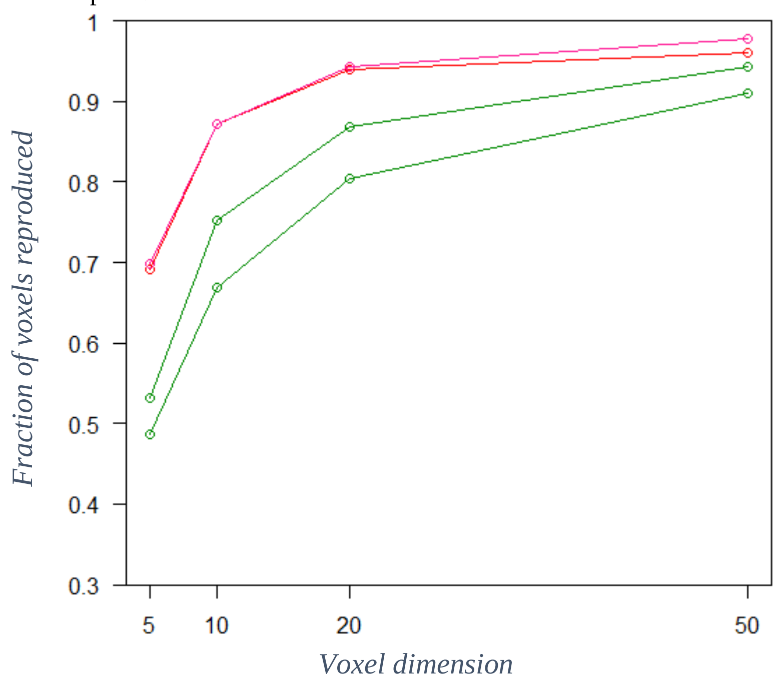

Conclusions

A priori understanding of the strengths and limitations of TLS sampling methods is vital to maximizing efficiency of sampling in logistically-challenging field campaigns, and we hope that the body of information provided here will offer useful guidance to future researchers planning the application of similar methods and instruments in rangelands. An important qualifier to our results and recommendations is that they may only apply to study areas with similar landscape characteristics to those we sampled. Different vegetation structure, such as taller or more dense vegetation and more complex topography will increase shadowing problems and decrease reproducibility of limited TLS collection methodologies.

The measures employed in each of our experiments changed greatly depending on the composition of vegetation in the plots and the scale at which measurements were made. By stratifying results by both, we hope that future researchers may identify the results most pertinent to their own work. Advance knowledge of study area composition as well as the resolution, coverage, and sampling reproducibility that is useful in datasets, coupled with information detailing the quality of datasets which specific sampling methods may be expected to yield, may increase the efficiency and logistical ease of TLS collections.

3.4. Literature Cited

Brodu, N., & Lague, D. (2012). 3D terrestrial lidar data classification of complex natural scenes using a multi-scale dimensionality criterion: Applications in geomorphology. *ISPRS Journal of Photogrammetry and Remote Sensing*, *68*, 121-134.

Chasmer, L., Hopkinson, C., & Treitz, P. (2004). Assessing the three-dimensional frequency distribution of airborne and ground-based lidar data for red pine and mixed deciduous forest plots. *The International Archives of the Photogrammetry, Remote Sensing and Spatial Information Sciences*, *36*, 8.

Clawges, R., Vierling, L., Calhoon, M., & Toomey, M. (2007). Use of a ground-based scanning lidar for estimation of biophysical properties of western larch (Larix occidentalis). *International Journal of Remote Sensing*, *28*(19), 4331-4344.

Coveney, S., & Stewart Fotheringham, A. (2011). Terrestrial laser scan error in the presence of dense ground vegetation. *The Photogrammetric Record*, *26*(135), 307-324.

Fan, L., Powrie, W., Smethurst, J., Atkinson, P. M., & Einstein, H. (2014). The effect of short ground vegetation on terrestrial laser scans at a local scale. *ISPRS Journal of Photogrammetry and Remote Sensing*, *95*, 42-52.

Henning, J. G., & Radtke, P. J. (2006). Ground-based laser imaging for assessing three-dimensional forest canopy structure. *Photogrammetric Engineering & Remote Sensing*, *72*(12), 1349-1358.

Heritage, G., & Large, A. (2009). *Laser scanning for the environmental sciences*. Hoboken, NJ: John Wiley & Sons.

Murgoitio, J, Shrestha, R, Glenn, N, and Spaete, L. (2014). Airborne LiDAR and terrestrial laser scanning derived vegetation obstruction factors for visibility models. *Transactions in GIS*, *18*(1): 147-160.

Loudermilk, E. L., Hiers, J. K., O'Brien, J. J., Mitchell, R. J., Singhania, A., Fernandez, J. C., Cropper, W.P. & Slatton, K. C. (2009). Ground-based LIDAR: a novel approach to quantify fine-scale fuelbed characteristics. *International Journal of Wildland Fire*, *18*(6), 676-685.

Olsoy, P. J., Glenn, N. F., Clark, P. E., & Derryberry, D. R. (2014). Aboveground total and green biomass of dryland shrub derived from terrestrial laser scanning. *ISPRS Journal of Photogrammetry and Remote Sensing*, *88*, 166-173.

Seidel, D., Fleck, S., & Leuschner, C. (2012). Analyzing forest canopies with ground-based laser scanning: A comparison with hemispherical photography. *Agricultural and Forest Meteorology*, *154*, 1-8.

Shan, J., & Toth, C. K. (2008). Topographic laser ranging and scanning: principles and processing. *CRC Press*.

Strahler, A. H., Jupp, D. L., Woodcock, C. E., Schaaf, C. B., Yao, T., Zhao, F., Yang, X., Lovell, J., Culvenor, D., Newnham, G., Ni-Miester, W., & Boykin-Morris, W. (2008). Retrieval of forest structural parameters using a ground-based lidar instrument (Echidna®). *Canadian Journal of Remote Sensing*, *34*(2), 426-440.

USDI Bureau of Land Management. (2008). *Snake River Birds of Prey National Conservation Area Proposed Resource Management Plan and Final Environmental Impact Statement*, *Boise*, *Idaho*.

Van der Zande, D., Jonckheere, I., Stuckens, J., Verstraeten, W. W., & Coppin, P. (2008). Sampling design of ground-based lidar measurements of forest canopy structure and its effect on shadowing. *Canadian Journal of Remote Sensing*, *34*(6), 526-538.

Vierling, L. A., Xu, Y., Eitel, J. U., & Oldow, J. S. (2013). Shrub characterization using terrestrial laser scanning and implications for airborne LiDAR assessment. *Canadian Journal of Remote Sensing*, *38*(6), 709-722.

Western Region Climate Center. 2012. *Swan Falls Power House*, *Idaho*, *Period of Record General Climate Summary*.
Retrieved from: http://www.wrcc.dri.edu/cgi-bin/cliMAIN.pl?id8928

Chapter 4: Conclusions

TLS was used to collect high-resolution structural data at 26 square hectare plots in rangelands in southwest Idaho. The resultant datasets were used as the basis of two studies: (1) an effort to predict the canopy cover and biomass of different morphological classes of vegetation, and (2) a series of experiments designed to quantify "shadowing" effects in TLS point clouds collected in rangelands and the success of methods to mitigate them. In combination, these studies form a foundation for the design of efficient and effective methods for rangeland vegetation inventory using TLS.

In Chapter 2, we show that pixel statistics about point cloud 3D structure serve as effective predictors of class-wise canopy cover fraction and biomass in models constructed using the Random Forests ensemble learning/decision trees algorithm. Using manual measurements taken at 9 systematically-placed 1 x 1 m quadrats at each plot (n = 206 after discarding plots with exceptionally poor TLS sampling coverage) for training and validation data, we modeled canopy cover fraction of annual grasses, perennial grasses, forbs, bare earth/litter, and shrubs, and biomass of herbaceous vegetation and shrubs with model strength ranging between $R^2 = 0.28$ and $R^2 = 0.72$. Our successful use of pixel statistics to infer vegetation characteristics expand on the known capabilities of TLS collections in rangelands, which have been previously used to predict height, crown area (Vierling et al. 2013), and biomass (Olsoy et al. 2014a,b) of individual sagebrush shrubs.

The successful use of pixel statistics as predictors of vegetation characteristics shows that vegetation inventory may be successfully performed without explicitly delineating and classifying individual plants. This approach is particularly useful when complementary manual sampling is performed on a per-area basis (rather than per-plant), and when individual plants cannot readily be delineated in laser scan point clouds (e.g. cheatgrass or clumped shrubs).

Intuitively, there is a trade-off between the resilience of statistics calculated using large pixels to small shadowed areas and stochastic flaws in point clouds, and the level of detail captured by calculating structural statistics at smaller pixel sizes. We found that the size of pixels used to calculate structural statistics did affect the strength of resultant models, and that the optimal pixel size varied among field measurements being predicted. Future studies should likewise test various pixel sizes for calculation of structural statistics to determine which yields the most powerful predictors of each variable.

There are several disadvantages to modeling vegetation characteristics based purely on pixel statistics of structure. These disadvantages include the weakening of allometric inference when a single biomass measurement describes either several plants combined or only portions of plants, as well as the loss of information about the spatial distribution of structure when pixel values from throughout a quadrat are aggregated into a single statistic. Beyond these inherent methodological challenges, we observed a number of common sampling errors in data collection, including small mistakes in co-location of manually-sampled data to TLS point clouds, canopy cover measurements which described extents larger than paired regions in TLS point clouds, inexact biomass sampling of large shrubs, and shadowed regions in TLS point clouds.

That the Random Forests algorithm yielded good quality models in spite of these difficulties is a testament to the power of machine learning methods to derive useful information from complex datasets. Starting with 145 predictors (per-quadrat mean, maximum, minimum, standard deviation, and a range of 29 structural statistics), Random Forests yielded strong models of each manually-measured characteristic using 4 or fewer TLS-derived predictors.

There are several immediate applications of the ability to accurately inventory vegetation classes over large rangeland plots. Urgent problems in the western USA stemming from altered regimes of wildfire and succession require efficient means of vegetation inventory to document baselines of ecosystem composition and evaluate the success of landscape treatment efforts using time series. The ability to inventory vegetation across large rangeland plots may also lend itself to numerous research and management purposes in drylands, which face a host of degradation problems worldwide. Ecological models that require input data in the form of simulated vegetation landscapes could use TLS to create fine-scale models which precisely replicate real-world conditions. Interpretation of aerial or satellite-based remote sensing, which has thus far been challenged in rangeland ecosystems, may be improved using broad-scale training data collected using TLS.

In Chapter 3, we carried out a series of experiments to better understand the limitations of TLS sampling in rangeland ecosystems, contributing to the small body of work that explicitly addresses methods to optimize quality and efficiency of TLS collections. We tested the effect of range-from-scanner on the extent of shadowed regions in datasets, the effectiveness of multiple scanning positions at reducing total shadowed area in 1 ha plots, and the reproducibility of point clouds yielded by a methodology employing 5 scans per hectare. We compared the differences in datasets yielded from shrub-dominated and grass-dominated plots, and the effect of different scales of measurement on statistics of sampling coverage and reproducibility. Unsurprisingly, each of our experiments showed that grass-dominated plots are less prone to shadowing problems than shrub-dominated plots, and that coarser scales of measuring sampling presence-absence indicated superior sampling coverage.

In testing the effect of range from scanning position on the fractional extent of unsampled regions in datasets, we found that the range of highly-effective sampling (> 90%) coverage extended some considerable distance out from the scan position, with this distance depending on the plot cover type and scale at which measurements were made. We found that very fine, low-lying vegetation was a significant mechanism of shadowing beyond short ranges, indicating that scanner height and plot vegetation composition (as opposed to scanning density) are the limiting factors of collection quality.

Examining the contribution to sampling coverage over 1 ha plots that was provided by successively-larger arrangements of scanning positions, we found that each of at least 5 positions contributed additional coverage when measurements of sampling coverage were made at fine (5 cm) scales. We showed that as many as 9 scan positions per hectare may be required to yield complete fine-scale sampling coverage in grassy plots, and that greater than 9 positions per hectare would be required to yield complete fine-scale sampling coverage in shrubby plots. However, when measurements of sampling coverage were coarsened to the 50 cm scale, 5 scan positions per hectare were sufficient to yield complete coverage in shrubby plots and 3 positions were sufficient in grassy plots.

Examining the rate of reproducibility among datasets yielded using a 5 scan position per hectare protocol, we found that implementations of this layout with the maximum difference in alignment yielded datasets which reproduced one another with rates ranging between 50% and 75% at fine scales (5 cm) and better than 90% at coarse scales (50 cm). These values are likely to be slightly optimistic estimations of actual reproducibility of datasets collected across hectare plots, as the actual area of consideration was 8283 m^2, and excluded plot corners; but pessimistic in that they are drawn from the most extreme case of positional separation between two different deployments of the scan position layout around a given centerpoint.

Although we do make general recommendations based on our results in Chapter 3 (e.g. the efficiency of collections may be optimized by spacing apart scan positions at least twice the distance at which very good sampling coverage is achieved), we intend researchers to draw their own conclusions from the information we provide. Pairing our results with advance awareness of field conditions and desired dataset quality, researchers may make educated decisions about the TLS collection effort worth investing at each site.

In combination, these studies present information about both how to optimize efficiency and sampling quality of TLS collections in rangelands, and how to effectively apply TLS data to inventory biomass and canopy cover of several rangeland vegetation types. Future work could immediately build on these studies by using TLS data to inventory grassland and shrubland vegetation based on collections performed using the guidance we provide to optimize TLS methods in rangelands. Terrestrial laser scanning-based predictions of vegetation characteristics could be strengthened further by collecting datasets which are functionally-free of lateral occlusion. Although we have not yet demonstrated methods to achieve this in shrub-dominated plots, it could be accomplished using scan positions which are more elevated or numerous than in the configuration we used. As it stands, our work is a proof-of-concept of TLS as an efficient and accurate tool of rangeland vegetation inventory, with immediate applicability to complement and extend management-oriented vegetation sampling already being performed in rangelands of the western USA.

Literature Cited

Adams, T. (2014). Using Terrestrial LiDAR to Model Shrubs for Fire Behavior Simulation.
Retrieved from: http://scholarworks.umt.edu/etd/4173/

Andariese, S. W., & Covington, W. W. (1986). Biomass estimation for four common grass species in northern Arizona ponderosa pine. *Journal of Range Management*, *39*(5), 472-473.

Andersen, H. E., McGaughey, R. J., & Reutebuch, S. E. (2005). Estimating forest canopy fuel parameters using LIDAR data. *Remote sensing of Environment*, *94*(4), 441-449.

Baker, W. L. (2011.) Pre-EuroAmerican and recent fire in sagebrush ecosystems. In: Ecology and conservation of Greater Sage-grouse: a landscape species and its habitats. *Studies in Avian Biology, 38*. Berkely, CA: University of California Press.

Balch, J. K., Bradley, B. A., D'Antonio, C. M., & Gómez-Dans, J. (2013). Introduced annual grass increases regional fire activity across the arid western USA (1980–2009). *Global Change Biology*, *19*(1), 173-183.

Beck, J. L., Connelly, J. W., & Reese, K. P. (2009). Recovery of greater sage-grouse habitat features in Wyoming big sagebrush following prescribed fire. *Restoration Ecology*, *17*(3), 393-403.

Bistinas, I., Oom, D., Sá, A. C., Harrison, S. P., Prentice, I. C., & Pereira, J. M. (2013). Relationships between Human Population Density and Burned Area at Continental and Global Scales. *PloS One*, *8*(12), e81188.

Bonham, C. D. (1989). *Measurements for terrestrial vegetation*. New York, NY: John Wiley and Sons.

Bork, E. W., & Su, J. G. (2007). Integrating LIDAR data and multispectral imagery for enhanced classification of rangeland vegetation: A meta analysis. *Remote Sensing of Environment*, *111*(1), 11-24.

Bregas, J. P. (1998). Ecological impacts of global change on drylands and their implications for desertification. *Land Degradation & Development*, *9*, 393-406.

Breiman, L. (2001). Random forests. *Machine Learning*, *45*(1), 5-32.

Breiman, L. (1996). Out-of-bag estimation. *Technical report 1996b*. Berkeley, CA: Statistics Department, University of California Berkeley.

Brodu, N., & Lague, D. (2012). 3D terrestrial lidar data classification of complex natural scenes using a multi-scale dimensionality criterion: Applications in geomorphology. *ISPRS Journal of Photogrammetry and Remote Sensing*, *68*, 121-134.

Brooks, M. L., D'antonio, C. M., Richardson, D. M., Grace, J. B., Keeley, J. E., DiTomaso, J. M., Hobbs, R.J, Pellant, M., & Pyke, D. (2004). Effects of invasive alien plants on fire regimes. *BioScience*, *54*(7), 677-688.

Bukowski, B. E., & Baker, W. L. (2013). Historical fire regimes, reconstructed from land-survey data, led to complexity and fluctuation in sagebrush landscapes. *Ecological Applications*, *23*(3), 546-564.

Chasmer, L., Hopkinson, C., & Treitz, P. (2004). Assessing the three-dimensional frequency distribution of airborne and ground-based lidar data for red pine and mixed deciduous forest plots. *The International Archives of the Photogrammetry, Remote Sensing and Spatial Information Sciences*, *36*, 8.

Clawges, R., Vierling, L., Calhoon, M., & Toomey, M. (2007). Use of a ground-based scanning lidar for estimation of biophysical properties of western larch (Larix occidentalis). *International Journal of Remote Sensing*, *28*(19), 4331-4344.

Coveney, S., & Stewart Fotheringham, A. (2011). Terrestrial laser scan error in the presence of dense ground vegetation. *The Photogrammetric Record*, *26*(135), 307-324.

Cowie, A. L., Penman, T. D., Gorissen, L., Winslow, M. D., Lehmann, J., Tyrrell, T. D., Twomlow, S., Wilkes, A., Lal, R., Jones, J.W., Paulsch, A., Kellner, K., & Akhtar-Schuster, M. (2011). Towards sustainable land management in the drylands: scientific connections in monitoring and assessing dryland degradation, climate change and biodiversity. *Land Degradation & Development*, *22*(2), 248-260.

D'Antonio, C. M., & Vitousek, P. M. (1992). Biological invasions by exotic grasses, the grass/fire cycle, and global change. *Annual Review of Ecology and Systematics*, 63-87.

Davies, K. W., & Bates, J. D. (2010). Vegetation characteristics of mountain and Wyoming big sagebrush plant communities in the northern Great Basin. *Rangeland Ecology & Management*, *63*(4), 461-466.

Davies, K. W., Bates, J. D., & Nafus, A. M. (2012). Vegetation response to mowing dense mountain big sagebrush stands. *Rangeland Ecology & Management*, *65*(3), 268-276.

Davison, J., & Smith, E. (1997). Greenstrips: another tool to manage wildfire. *University of Nevada Cooperative Extension Fact Sheet*, *36*.

Estornell, J., Ruiz, L. A., Velázquez-Martí, B., & Fernández-Sarría, A. (2011). Estimation of shrub biomass by airborne LiDAR data in small forest stands. *Forest ecology and management*, *262*(9), 1697-1703.

Fan, L., Powrie, W., Smethurst, J., Atkinson, P. M., & Einstein, H. (2014). The effect of short ground vegetation on terrestrial laser scans at a local scale. *ISPRS Journal of Photogrammetry and Remote Sensing*, *95*, 42-52.

Garrity, S. R., Meyer, K., Maurer, K. D., Hardiman, B., & Bohrer, G. (2012). Estimating plot-level tree structure in a deciduous forest by combining allometric equations, spatial wavelet analysis and airborne LiDAR. *Remote Sensing Letters*, *3*(5), 443-451.

Goudie, A. S. (2014). Desert dust and human health disorders. *Environment International*, *63*, 101-113.

Henning, J. G., & Radtke, P. J. (2006). Ground-based laser imaging for assessing three-dimensional forest canopy structure. *Photogrammetric Engineering & Remote Sensing*, *72*(12), 1349-1358.

Heritage, G., & Large, A. (2009). *Laser scanning for the environmental sciences*. Hoboken, NJ: John Wiley & Sons.

Hess, J. E., & Beck, J. L. (2012). Burning and mowing Wyoming big sagebrush: Do treated sites meet minimum guidelines for greater sage-grouse breeding habitats? *Wildlife Society Bulletin*, *36*(1), 85-93.

Hopkinson, C., Chasmer, L. E., Sass, G., Creed, I. F., Sitar, M., Kalbfleisch, W., & Treitz, P. (2005). Vegetation class dependent errors in lidar ground elevation and canopy height estimates in a boreal wetland environment. *Canadian Journal of Remote Sensing*, *31*(2), 191-206.

Hudak, A. T., Crookston, N. L., Evans, J. S., Hall, D. E., & Falkowski, M. J. (2008). Nearest neighbor imputation of species-level, plot-scale forest structure attributes from LiDAR data. *Remote Sensing of Environment*, *112*(5), 2232-2245.

Hunt, E. R., Kelly, R. D., Smith, W. K., Fahnestock, J. T., Welker, J. M., & Reiners, W. A. (2004). Estimation of carbon sequestration by combining remote sensing and net ecosystem exchange data for northern mixed-grass prairie and sagebrush–steppe ecosystems. *Environmental Management*, *33*(1), 432-441.

Jacobson, J. E., & Snyder, M. C. (2000). Shrubsteppe mapping of eastern Washington using Landsat satellite Thematic Mapper data. *Spatial Data Management Section*. Science Division, Wildlife Program, Washington Department of Fish and Wildlife.

Johnson, D. D., & Davies, K. W. (2012). Medusahead management in sagebrush-steppe rangelands: prevention, control, and revegetation. *Rangelands*, *34*(1), 32-38.

Kałuża, T., Tymków, P., & Strzeliński, P. (2012). Use of remote sensing for investigating riparian shrub structures. *Polish Journal of Environmental Studies*, *21*(1).

Knick, S. T. (1999). Requiem for a sagebrush ecosystem? *Northwest Science*, *73*(1).

Knick, S. T., Hanser, S. E., Miller, R. F., Pyke, D. A., Wisdom, M. J., Finn, S. P., Rinkes E.T. & Henny, C. J. (2011). Ecological influence and pathways of land use in sagebrush. *Studies in Avian Biology*, *38*, 203-251.

Knick, S. T., Rotenberry, J. T., & Zarriello, T. J. (1997). Supervised classification of Landsat Thematic Mapper imagery in a semi-arid rangeland by nonparametric discriminant analysis. *Photogrammetric Engineering and Remote Sensing*, *63*(1), 79-86.

Knick, S. T., Schroeder, M. A., & Stiver, S. J. (2004). *Conservation assessment of greater sage-grouse and sagebrush habitats.* Cheyenne, WY: Western Association of Fish and Wildlife Agencies.

Kuhn, M. (2008). Building predictive models in R using the caret package. *Journal of Statistical Software*, *28*(5), 1-26.

Li, A., Glenn, N.F., Olsoy, P.J., Mitchell, J.J., Shrestha, R. 2014. Scaling aboveground biomass estimates of sagebrush using terrestrial and airborne LiDAR data in a dryland ecosystem. *Agricultural and Forest Meteorology* (in review).

Loudermilk, E. L., Hiers, J. K., O'Brien, J. J., Mitchell, R. J., Singhania, A., Fernandez, J. C., Cropper, W.P. & Slatton, K. C. (2009). Ground-based LIDAR: a novel approach to quantify fine-scale fuelbed characteristics. *International Journal of Wildland Fire*, *18*(6), 676-685.

Miller, R. F., & Eddleman, L. (2000). *Spatial and temporal changes of sage grouse habitat in the sagebrush biome*. Corvallis, OR: Oregon State University, Agricultural Experiment Station.

Miller, R. F. & Heyerdahl, E. K. (2008). Fine-scale variation of historical fire regimes in sagebrush-steppe and juniper woodland: an example from California, USA. *International Journal of Wildland Fire*, *17*, 245-254.

Miller, R. F., & Rose, J. A. (1999). Fire history and western juniper encroachment in sagebrush steppe. *Journal of Range Management*, 550-559.

Miller, R. F., & Tausch, R. J. (2000). The role of fire in pinyon and juniper woodlands: a descriptive analysis. *Proceedings of the invasive species workshop: the role of fire in the control and spread of invasive species*. *Fire Conference 2000: the First National Congress on Fire Ecology, Prevention, and Management.*

Milton, S. J., Dean, W. R. J., du Plessis, M. A., & Siegfried, W. R. (1994). A conceptual model of arid rangeland degradation. *BioScience*, 70-76.

Mitchell, J. J., Glenn, N. F., Sankey, T. T., Derryberry, D. R., Anderson, M. O., & Hruska, R. C. (2011). Small-footprint LiDAR estimations of sagebrush canopy characteristics. *Photogrammetric Engineering & Remote Sensing*, *77*(5), 521-530.

Mitchell, J., Shrestha, R., Spaete, L.P., Glenn, N.F. (2014). Combining airborne LiDAR and hyperspectral data across local sites for upscaling shrubland structural information: lessons for HyspIRI. *Remote Sensing of Environment* (in review).

Mundt, J. T., Streutker, D. R., & Glenn, N. F. (2006). Mapping sagebrush distribution using fusion of hyperspectral and lidar classifications. *Photogrammetric Engineering & Remote Sensing*, *72*(1), 47-54.

Murgoitio, J, Shrestha, R, Glenn, N, and Spaete, L. (2014). Airborne LiDAR and terrestrial laser scanning derived vegetation obstruction factors for visibility models. *Transactions in GIS*, *18*(1): 147-160.

Northwest Power and Conservation Council. (2004). *Upper Snake subbasin assessment*. Portland, Oregon: Northwest Power and Conservation Council.

Okin, G. S., Roberts, D. A., Murray, B., & Okin, W. J. (2001). Practical limits on hyperspectral vegetation discrimination in arid and semiarid environments. *Remote Sensing of Environment*, *77*(2), 212-225.

Olsoy, P, N Glenn, & Clark, P. (2014). Estimating sagebrush biomass using terrestrial laser scanning (TLS). *Rangeland Ecology & Management*, *67* (2): 224-228.

Olsoy, P. J., Glenn, N. F., Clark, P. E., & Derryberry, D. R. (2014). Aboveground total and green biomass of dryland shrub derived from terrestrial laser scanning. *ISPRS Journal of Photogrammetry and Remote Sensing*, *88*, 166-173.

Olsoy, P.J., Forbey, J.S., Rachlow, J.L., Nobler, J.D., Glenn, N.F., & Shipley, L.A. (2014). Fearscapes: Mapping functional properties of cover for prey with terrestrial LiDAR. *Bioscience* (in press).

Ravi, S., Breshears, D. D., Huxman, T. E., & D'Odorico, P. (2010). Land degradation in drylands: Interactions among hydrologic–aeolian erosion and vegetation dynamics. *Geomorphology*, *116*(3), 236-245.

Reynolds, J. F., Maestre, F. T., Kemp, P. R., Stafford-Smith, D. M., & Lambin, E. (2007). Natural and human dimensions of land degradation in drylands: causes and consequences. *Terrestrial ecosystems in a changing world*. Berlin, Germany: Springer.

Sankey, J. B., Germino, M. J., Benner, S. G., Glenn, N. F., & Hoover, A. N. (2012). Transport of biologically important nutrients by wind in an eroding cold desert. *Aeolian Research*, *7*, 17-27.

Sankey, T. T., & Bond, P. (2011). LiDAR-based classification of sagebrush community types. *Rangeland Ecology and Management*, *64*(1), 92-98.

Sankey, T. T., & Germino, M. J. (2008). Assessment of juniper encroachment with the use of satellite imagery and geospatial data. *Rangeland Ecology & Management*, *61*(4), 412-418.

Sankey, T. T., Glenn, N., Ehinger, S., Boehm, A., & Hardegree, S. (2010). Characterizing western juniper expansion via a fusion of Landsat 5 Thematic Mapper and lidar data. *Rangeland Ecology & Management*, *63*(5), 514-523.

Seidel, D., Fleck, S., & Leuschner, C. (2012). Analyzing forest canopies with ground-based laser scanning: A comparison with hemispherical photography. *Agricultural and Forest Meteorology*, *154*, 1-8.

Seielstad, C., Stonesifer, C., Rowell, E., & Queen, L. (2011). Deriving fuel mass by size class in Douglas-fir (Pseudotsuga menziesii) using terrestrial laser scanning. *Remote Sensing*, *3*(8), 1691-1709.

Shan, J., & Toth, C. K. (2008). Topographic laser ranging and scanning: principles and processing. *CRC Press*.

Shinneman, D., Arkle, R., Pilliod, D., Glenn, N.F. (2011). Quantifying and predicting fuels and the effects of reduction treatments along successional and invasion gradients in sagebrush habitats.
Retrieved from:
http://www.firescience.gov/JFSP_funded_project_detail.cfm?jdbid=%24%26ZO9V0%20%20%0A

Strahler, A. H., Jupp, D. L., Woodcock, C. E., Schaaf, C. B., Yao, T., Zhao, F., Yang, X., Lovell, J., Culvenor, D., Newnham, G., Ni-Miester, W., & Boykin-Morris, W. (2008). Retrieval of forest structural parameters using a ground-based lidar instrument (Echidna®). *Canadian Journal of Remote Sensing*, *34*, 426-440.

Streutker, D. R., & Glenn, N. F. (2006). LiDAR measurement of sagebrush steppe vegetation heights. *Remote Sensing of Environment*, *102*(1), 135-145.

Tausch, R. J. (1989). Comparison of regression methods for biomass estimation of sagebrush and bunchgrass. *Western North American Naturalist*, *49*(3), 373-380.

U.S. Army Engineer Research and Development Center. (2012). TEC Tests Mast-Mounted LiDAR for Deployable Force Protection at MSCoE-CBITEC Forward Operating Base.
Retrieved from:
http://www.erdc.usace.army.mil/Media/NewsStories/tabid/9219/Article/476222/tec-tests-mast-mounted-lidar-for-deployable-force-protection-at-mscoecbitec-for.aspx

Uresk, D. W., Gilbert, R. O., & Rickard, W. H. (1977). Sampling big sagebrush for phytomass. *Journal of Range Management*, 311-314.

USDI Bureau of Land Management. (2008). *Snake River Birds of Prey National Conservation Area Proposed Resource Management Plan and Final Environmental Impact Statement, Boise, ID*.

Van der Zande, D., Jonckheere, I., Stuckens, J., Verstraeten, W. W., & Coppin, P. (2008). Sampling design of ground-based lidar measurements of forest canopy structure and its effect on shadowing. *Canadian Journal of Remote Sensing*, *34*(6), 526-538.

Vierling, K. T., Vierling, L. A., Gould, W. A., Martinuzzi, S., & Clawges, R. M. (2008). Lidar: shedding new light on habitat characterization and modeling. *Frontiers in Ecology and the Environment*, *6*(2), 90-98.

Vierling, L. A., Xu, Y., Eitel, J. U., & Oldow, J. S. (2013). Shrub characterization using terrestrial laser scanning and implications for airborne LiDAR assessment. *Canadian Journal of Remote Sensing*, 38(6), 709-722.

Welch, B. L. (2005). Big sagebrush: a sea fragmented into lakes, ponds, and puddles. *General Technical Report 144*. Fort Collins, CO, USA: US Department of Agriculture, Forest Service, Rocky Mountain Research Station.

Western Region Climate Center. 2012. Swan Falls Power House, Idaho, Period of Record General Climate Summary.
Retrieved from: http://www.wrcc.dri.edu/cgi-bin/cliMAIN.pl?id8928

White, R. P., & Nackoney, J. (2003). Drylands, People, and Ecosystem Goods and Services: A Web-based Geospatial Analysis. World Resources Institute.
Retrieved from: http://pdf.wri.org/drylands.pdf

World Resources Institute. (2005). Ecosystems and human well-being: desertification synthesis. *Millennium Ecosystem Assessment*.

Wulder, M. A., White, J. C., Nelson, R. F., Næsset, E., Ørka, H. O., Coops, N. C., Hilker, T., Bater, C.W., & Gobakken, T. (2012). Lidar sampling for large-area forest characterization: A review. *Remote Sensing of Environment*, *121*, 196-209.

Yao, T., Yang, X., Zhao, F., Wang, Z., Zhang, Q., Jupp, D., Lovell, J., Culvenor, D., Newnham, G., Ni-Meister, W., Schaaf, C., Woodcock, C., Wang, J., Li, X., & Strahler, A. (2011). Measuring forest structure and biomass in New England forest stands using Echidna ground-based lidar. *Remote sensing of Environment*, *115*(11), 2965-2974.

Zhao, F., Strahler, A. H., Schaaf, C. L., Yao, T., Yang, X., Wang, Z., Schull, M.A., Román-Colón, M.O., Woodcock, C.E., Olofsson, P., Ni-Meister, W., Jupp, D.L.B., Lovell, J.L., Culvenor, D.S., & Newnham, G. J. (2012). Measuring gap fraction, element clumping index and LAI in Sierra Forest stands using a full-waveform ground-based lidar. *Remote Sensing of Environment*, *125*, 73-79.

Zhao, F., Yang, X., Schull, M. A., Román-Colón, M. O., Yao, T., Wang, Z., Yao, T., Wang, Z., Zhang, Q., Jupp, D.L.B., Lovell, J.L., Culvenor, D.S., Newnham, G.J., Richardson, A.D., Ni-Meister, W., Schaaf, C.L., Woodcock, C.E., & Strahler, A. H. (2011). Measuring effective leaf area index, foliage profile, and stand height in New England forest stands using a full-waveform ground-based lidar. *Remote Sensing of Environment*, *115*(11), 2954-2964.

Appendices

Table A.1. Optimal Random Forest models produced by each combination of input parameters and quality score. N describes the number of predictor variables used. These models were created using the R library caret (Kuhn 2008), which enables automated selection of optimal models. Although models tend to be slightly weaker than those yielded by Salford Predictive Modeler, this table illustrates the change in predictive power with number of variables (Chapter 2).

		5 cm window			**10 cm window**			**20 cm window**		
Feature	**Score**	R^2	RMSE	N	R^2	RMSE	N	R^2	RMSE	N
Shrub cover	1	0.59	8.8 %	4	0.54	9.3 %	4	0.56	9.1 %	5
	2	0.59	8.5 %	4	0.52	9.3 %	2	0.54	9.1 %	4
	3	0.64	5.9 %	5	0.67	5.7 %	5	0.65	5.8 %	1
Bare earth/litter cover	1	0.41	21.2 %	3	0.42	21.2 %	2	0.40	21.0 %	4
	2	0.41	21.3 %	2	0.41	21.4 %	1	0.40	21.0 %	4
	3	0.05	25.1 %	5	0.14	23.5 %	5	0.04	25.7 %	3
Annual grass cover	1	0.61	24.0 %	3	0.60	24.3 %	2	0.58	25.2 %	1
	2	0.62	23.3 %	4	0.58	25.3 %	1	0.61	23.7 %	4
	3	0.23	27.7 %	4	0.28	27.1 %	2	0.28	27.1 %	3
Perennial grass cover	1	0.23	13.5 %	5	0.26	13.2 %	3	0.23	13.6 %	2
	2	0.16	14.2 %	5	0.23	13.6 %	4	0.14	14.6 %	2
	3	0.01	18.2 %	5	0.10	16.9 %	2	0.03	19.1 %	1
Forb cover	1	0.44	6.7 %	2	0.45	6.6 %	3	0.43	6.7 %	4
	2	0.50	6.3 %	4	0.46	6.6 %	3	0.45	6.6 %	4
	3	0.43	6.4 %	2	0.40	6.6 %	2	0.39	6.6 %	4
Herbaceous biomass	1	0.42	122.5 g	2	0.41	121.8 g	3	0.47	115.0 g	3
	2	0.14	127.2 g	2	0.17	122.3 g	2	0.12	128.3 g	4
	3	0.08	61.7 g	2	0.00	68.9 g	2	0.07	61.9 g	3
Shrub biomass	1	0.37	257.9 g	4	0.46	237.1 g	4	0.45	237.6 g	3
	2	0.33	222.4 g	4	0.28	236.8 g	3	0.29	228.5 g	4
	3	0.57	88.7 g	2	0.69	76.3 g	2	0.27	115.9 g	5

Table A.2. The sampling quality score assigned to each quadrat in the study. An "X" indicates that the quadrat was discarded. Quadrats were numbered in reading order from the Northwest (Chapter 2).

	Quadrat								
Plot	1	2	3	4	5	6	7	8	9
106	2	2	2	2	2	2	2	2	3
107	2	2	3	X	2	2	2	2	2
110	2	2	2	2	2	2	2	2	2
114	2	X	3	2	1	3	3	3	2
115	3	2	3	3	3	3	2	3	X
117	2	3	2	1	2	X	X	2	X
200	2	2	2	2	2	2	3	1	2
203	3	3	3	3	2	3	2	2	X
204	3	3	3	3	3	3	2	3	2
209	3	3	3	X	1	3	1	2	1
211	3	X	3	X	3	X	3	3	3
214	2	X	3	X	2	3	X	X	X
216	X	X	X	1	3	2	2	X	2
332	X	X	3	3	2	2	3	2	2
338	2	2	2	3	3	2	3	2	2
341	3	3	2	3	3	3	3	2	3
350	2	X	2	3	2	2	2	3	2
352	2	2	X	X	3	3	2	3	3
353	3	3	3	3	3	X	2	3	3
354	3	X	3	2	3	2	3	3	3
411	2	2	2	2	3	X	2	2	2
415	2	3	3	3	3	3	2	2	3
416	3	3	3	3	3	3	3	3	3
417	3	3	3	3	3	3	3	2	3
421	1	2	3	2	2	3	1	2	2
422	2	2	3	2	2	3	2	2	2

Table A.3. The dates between 5/15/2013 and 6/14/2013 at which TLS performed and the number of days until manual sampling was carried out (Chapter 2).

Plot	Date of TLS sampling	Days elapsed until manual sampling
106	5/16/2013	1
107	5/16/2013	1
110	5/15/2013	19
114	6/10/2013	136
115	6/6/2013	140
117	6/6/2013	14
200	6/11/2013	7
203	6/12/2013	6
204	6/12/2013	6
209	5/17/2013	18
211	5/15/2013	2
214	5/17/2013	32
216	5/17/2013	18
332	6/4/2013	142
338	6/13/2013	6
341	6/5/2013	141
350	6/14/2013	5
352	6/5/2013	141
353	6/14/2013	5
354	6/5/2013	141
411	5/23/2013	14
415	5/23/2013	13
416	5/24/2013	13
417	5/22/2013	20
421	6/10/2013	1
422	6/10/2013	1

Table A.4. Plot-wise statistics of the quadrat manual measurements modeled in the study (Chapter 2).

Plot	Descriptor	Shrub Cover (%)	Ground Cover (%)	Annual grass cover (%)	Perennial grass cover (%)	Forb cover (%)	Herbaceous biomass (g)	Shrub biomass (g)
106	Mean	0.0	10.8	84.3	0.4	4.3	274.1	0.0
	Standard deviation	0.0	21.8	30.2	1.0	8.7	99.1	0.0
107	Mean	0.0	13.0	80.4	2.9	3.6	197.2	0.0
	Standard deviation	0.0	21.9	22.5	2.5	4.1	83.4	0.0
110	Mean	0.8	10.7	84.5	3.8	0.2	117.9	1.9
	Standard deviation	2.3	9.7	9.8	4.2	0.4	24.3	5.5
114	Mean	30.1	56.2	1.4	12.0	0.3	258.1	245.1
	Standard deviation	22.5	16.6	1.6	12.7	0.4	301.6	408.5
115	Mean	0.0	33.9	29.7	15.9	20.4	159.2	0.0
	Standard deviation	0.0	20.4	26.2	19.2	7.4	86.8	0.0
117	Mean	16.6	58.5	11.8	12.4	0.7	272.6	300.1
	Standard deviation	10.1	18.8	11.0	17.4	1.5	214.5	395.0
200	Mean	3.8	28.5	59.8	7.9	0.0	99.0	57.5
	Standard deviation	7.1	27.6	34.3	9.6	0.0	64.4	125.6
203	Mean	0.0	38.7	48.9	12.3	0.3	93.1	0.0
	Standard deviation	0.0	26.1	26.9	9.4	0.7	82.6	0.0
204	Mean	0.0	40.4	46.3	12.2	1.2	130.6	8.4
	Standard deviation	0.0	26.5	27.7	14.1	1.5	42.9	23.9
209	Mean	0.0	26.2	62.5	11.3	0.0	123.6	0.0
	Standard deviation	0.0	20.4	25.8	7.4	0.0	57.2	0.0
211	Mean	0.0	27.4	55.5	15.4	1.7	68.5	0.0
	Standard deviation	0.0	22.8	35.6	12.2	3.7	24.6	0.0
214	Mean	0.0	7.4	83.3	9.3	0.0	210.4	5.3
	Standard deviation	0.0	9.4	11.9	7.0	0.0	87.5	9.1
216	Mean	0.0	40.9	34.6	24.5	0.2	170.8	1.3
	Standard deviation	0.0	18.4	16.1	7.1	0.4	85.9	2.6
332	Mean	23.8	73.2	1.0	1.7	0.3	47.6	226.2
	Standard deviation	7.6	11.6	2.5	2.1	0.5	35.2	146.1
338	Mean	30.3	47.0	0.1	19.9	2.9	111.5	847.0
	Standard deviation	13.9	9.5	0.3	10.9	2.3	51.2	787.5
341	Mean	0.0	57.2	0.0	24.4	18.5	72.0	0.0
	Standard deviation	0.0	17.1	0.0	14.4	6.4	33.3	0.0
350	Mean	15.1	58.6	0.0	2.1	24.2	137.5	131.4
	Standard deviation	13.4	18.0	0.0	4.9	20.3	110.0	228.1
352	Mean	14.9	69.5	1.0	11.2	3.5	30.2	0.0
	Standard deviation	23.3	19.2	1.7	11.0	3.8	27.0	0.0
353	Mean	1.1	71.4	0.0	21.8	5.6	48.6	8.8
	Standard deviation	0.9	15.1	0.0	18.2	6.0	13.6	15.1
354	Mean	19.7	62.8	0.0	17.0	0.5	53.3	104.0

	Standard deviation	8.7	15.4	0.0	16.5	1.0	47.1	170.5
411	Mean	1.4	6.4	91.3	0.8	0.0	196.6	11.3
	Standard deviation	3.8	9.5	12.7	1.1	0.0	78.3	29.9
415	Mean	5.0	14.0	76.7	4.3	0.0	192.7	104.7
	Standard deviation	13.4	10.4	19.4	3.0	0.0	108.9	296.2
416	Mean	0.0	46.0	26.9	21.6	5.5	88.4	0.0
	Standard deviation	0.0	11.8	20.8	11.1	11.0	39.3	0.0
417	Mean	0.0	52.4	1.1	45.6	0.9	79.5	0.0
	Standard deviation	0.0	17.8	3.2	19.5	1.6	41.3	0.0
421	Mean	7.8	55.3	23.3	12.5	2.8	489.4	404.4
	Standard deviation	11.0	16.0	19.2	12.7	5.1	382.4	656.3
422	Mean	23.9	49.9	3.6	22.2	0.3	87.6	183.8
	Standard deviation	10.3	11.4	3.7	8.5	0.7	26.0	144.3

Figure A.1. The distribution of residuals between modeled and measured values from each plot (n=26). Red and blue coloring is to assist differentiating alternating plots. Residuals from each plot tending to be randomly distributed around 0 suggests that quadrat measurements do not differ due to the plot they fall in, which would cause the model to consistently either over- or under-predict values from each plot (Chapter 2).

Feature	Chart of Residuals
Annual grass cover (%)	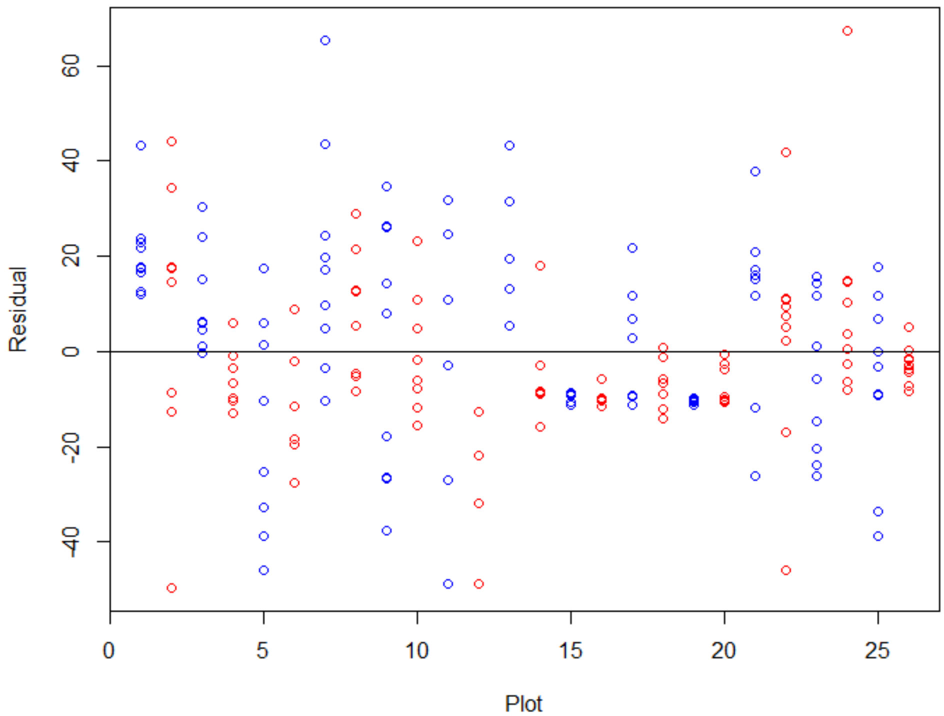
Bare earth/ litter cover (%)	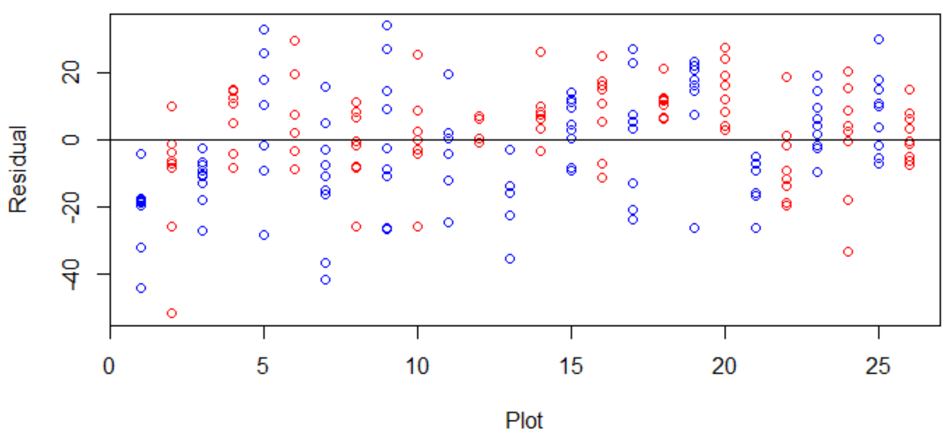

Forb cover (%)

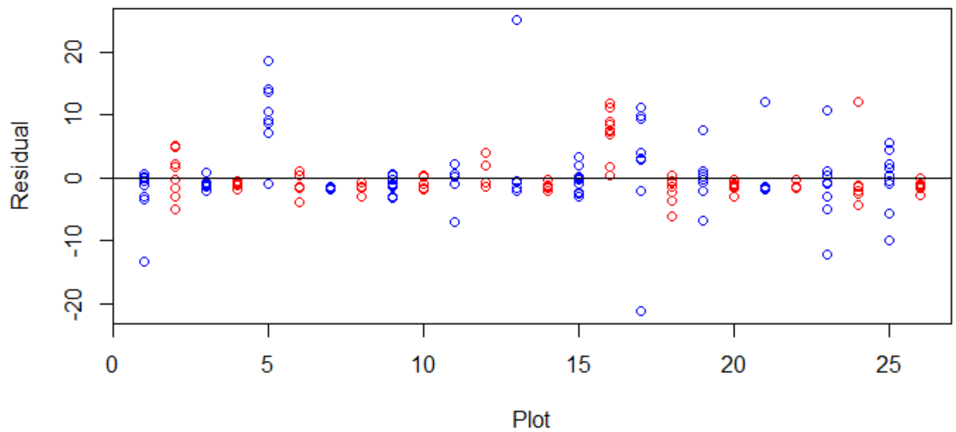

Perennial grass cover (%)

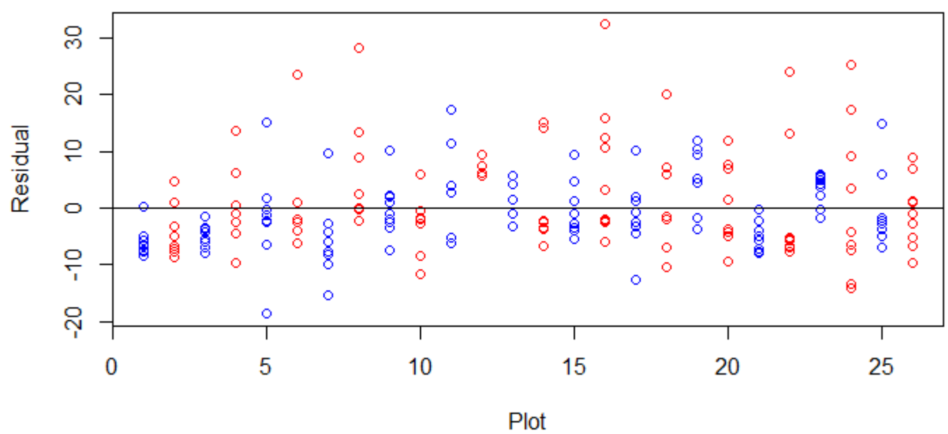

Shrub cover (%)

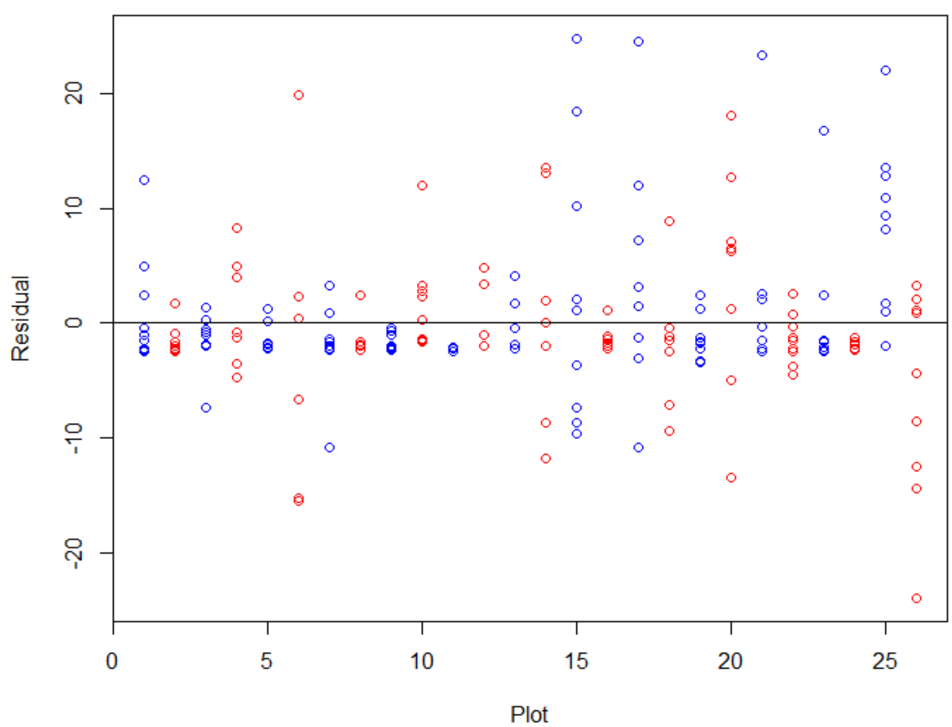

Herbaceous biomass (g)

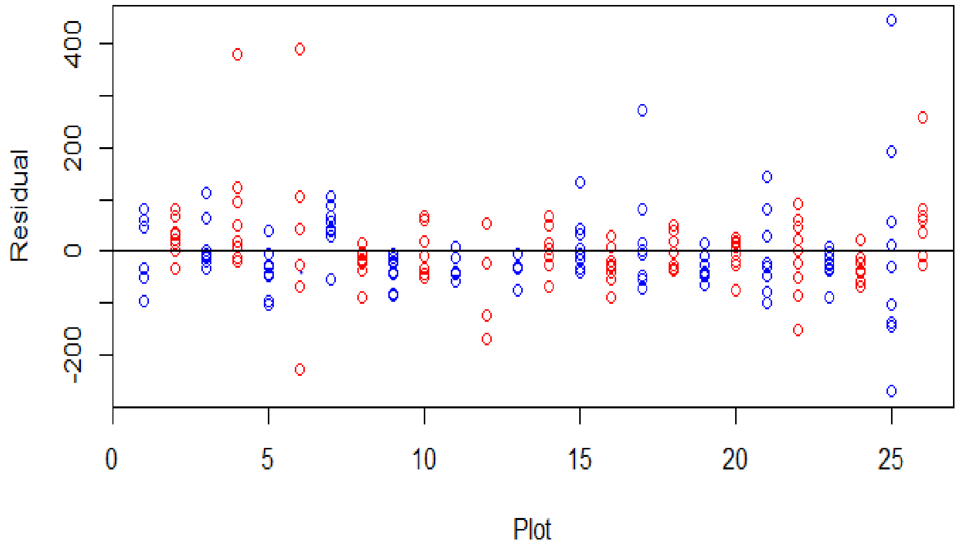

Shrub biomass (g)